DOI: 10.1002/ejoc.200500668

Synthesis and Conformational Analysis of Saturated *cis*-and *trans*-1,3,2-Benzodiazaphosphinine 2-Oxides

Zita Zalán,[a,b] Henri Kivelä,[a] László Lázár,[a,b] Ferenc Fülöp,*[b] and Kalevi Pihlaja*[a]

Keywords: Phosphorus heterocycles / Fused-ring systems / Structure elucidation / Configuration determination / Conformation analysis

By cyclization of *N*-unsubstituted, and N^1- or N^3-methyl-substituted *cis*- and *trans*-2-(aminomethyl)cyclohexylamines with phenylphosphonic dichloride, phenyl dichlorophosphate and bis(2-chloroethyl)phosphoramidic dichloride, P epimeric diastereomers **a** and **b** of the corresponding 1,3-unsubstituted and 1- or 3-methyl-substituted 2-phenyl-, 2-phenoxy- and 2-[bis(2-chloroethyl)amino]decahydro-1,3,2-benzodiazaphosphinine 2-oxides have been synthesized. The stereochemistry and conformations of the prepared saturated 1,3,2-benzodiazaphosphinine 2-oxides were determined by ^{1}H, ^{13}C and ^{31}P NMR spectroscopy aided by DFT geometry optimizations and *J*-coupling-constant calculations for selected structures. The 2-phenoxy-substituted *trans*-fused derivatives with an equatorial phenoxy group in a hypothetical double-chair conformation (**14a**, **16a**, **18a**) were observed to adopt nonchair heteroring conformations with a pseudoaxial P–OPh bond instead. The corresponding **b** epimers, as well as the *trans*-fused 2-phenyl and 2-[bis(2-chloroethyl)amino] derivatives (both P epimers) were found to retain double-chair conformations. In the *cis*-fused series, the position of the *N-in*/*N-out* equilibrium was dependent on the steric and stereoelectronic requirements of the phosphorus substituents (and thus on the phosphorus configuration) as well as on the substituents at the ring nitrogen atoms.

Introduction

As a consequence of their valuable pharmacological effects and synthetic utility, 1,3,2-oxazaphosphinane derivatives have attracted considerable interest. This ring system is found in alkylating anticancer drugs (cyclophosphamide, ifosfamide), numerous derivatives of which have been synthesized to determine their structure–activity relationships.[1] Alkylation of phosphorus-stabilized carbanions derived from 1,3,2-oxazaphosphinane 2-oxides have proved to be an efficient method for the diastereoselective construction of carbon–carbon bonds.[2,3]

However, the analogous 1,3,2-diazaphosphinane ring system has been less thoroughly studied either from a pharmacological or stereochemical point of view.[4] The 1,3,2-N,N,P analogue of cyclophosphamide was found to have no significant anticancer activity.[5] The synthetic importance of 1,3,2-N,N,P heterocycles increased when 1,3,2-diazaphosphinane phosphoramides proved to be effective auxiliaries with which to induce stereoselective carbon–carbon or carbon–hydrogen bond-forming reactions, for example, asymmetric aldol reactions,[6,7] allylations of aldehydes,[8] α-alkylations of *P*-alkyl derivatives[9] and reductions of ketones.[10] Stereochemical studies on some monocyclic and tetrahydroisoquinoline-condensed 1,3,2-diazaphosphinane 2-oxide model compounds have led to the conclusion that, in contrast to the conformationally diverse 1,3,2-oxazaphosphinane analogues, these compounds could be characterized by chair or twisted-chair conformations.[4,11]

As a continuation of our previous studies on cyclohexane-condensed phosphorus-containing 1,2,3-heterocycles,[12,13] our aim in this work was to prepare P epimeric diastereomers of *cis*- and *trans*-1,2,3,4,4a,5,6,7,8,8a-decahydro-1,3,2-benzodiazaphosphinine 2-oxides bearing substituents on the heteroatoms for the purpose of investigating the effects of the presence of these substituents and the relative configuration of the phosphorus atom on the predominant conformation of the saturated bicyclic system.

Results and Discussion

Synthesis

The methods applied earlier to the synthesis of 1,3,2-N,N,P heterocycles were based on the ring-closure of the corresponding diamines with the appropriate phosphorus-containing fragments.[4,14] The *cis* and *trans* cyclohexane 1,3-diamines **3a**,**b** and **4a**,**b** required for the cyclization reactions were prepared by lithium aluminium hydride re-

[a] Department of Chemistry, University of Turku, 20014 Turku, Finland
E-mail: kpihlaja@utu.fi
[b] Institute of Pharmaceutical Chemistry, University of Szeged, 6701 Szeged, POB 427, Hungary
E-mail: fulop@pharm.u-szeged.hu
Supporting information for this article is available on the WWW under http://www.eurjoc.org or from the author.

duction of the corresponding *cis*- and *trans*-2-aminocyclohexanecarboxamides (**1a**,**b** and **2a**,**b**) (Scheme 1).[15,16] Diamines **6a**,**b**, bearing a methyl substituent on the nitrogen atom adjacent to the cyclohexane ring, were synthesized by analogous reductions of the urethanes **5a**,**b** derived from carboxamides **1a**,**b**.

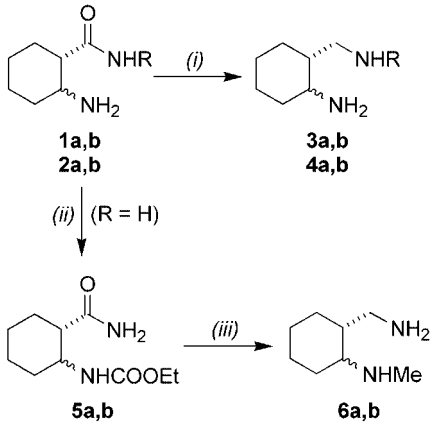

Scheme 1. Reagents and conditions: (*i*) $LiAlH_4$, THF, reflux, 12 h, 51% (**3a**), 55% (**3b**); see ref.[16] (**4a**,**b**); (*ii*) ClCOOEt, $NaHCO_3$, toluene, H_2O, room temp., 1 h, 75% (**5a**), 98% (**5b**); (*iii*) $LiAlH_4$, THF, reflux, 3 h, 43% (**6a**), 36% (**6b**). R = H: **1**, **3**; R = Me: **2**, **4**; *cis*: **a**; *trans*: **b**.

The cyclization reactions of the *cis* and *trans* diamines **3a**,**b**, **4a**,**b** and **6a**,**b** with phenylphosphonic dichloride, phenyl dichlorophosphate and bis(2-chloroethyl)phosphoramidic dichloride were performed at ambient temperature to give 1,2,3,4,4a,5,6,7,8,8a-decahydro-1,3,2-benzodiazaphosphinine 2-oxides **7**–**22** (Scheme 2 and Scheme 3). In all cases, two diastereomers (**a** and **b**) differing in the configuration of the phosphorus atom relative to the carbon atoms at the annelation positions were formed which, except for **20a**,**b**, could be separated by column chromatography. The ratios of the diastereomers formed were determined from the NMR spectra of the crude products (see Exp. Sect.).

Characterization of Structures

The solution-state structures and conformations of the prepared compounds **7**–**22a**,**b** in $CDCl_3$ were characterized by ^1H, ^{13}C and ^{31}P NMR spectroscopic methods at 25 °C. A limited conformational search followed by *J*-coupling-constant calculations on the geometry-optimized conformations was also undertaken for the epimeric pair **10a** and **10b** by using DFT methods.

The ^1H and ^{13}C NMR signals (see Tables 1, 2, 3, 4, 5, 6, and 7) were assigned with the help of standard 2D homo- and heteronuclear correlation methods (cf. Exp. Sect.). The signals from (diastereotopic) geminal methylene protons could be individually assigned based on their chemical shifts and/or *J* coupling constants: In the *trans*-fused series, axial protons (H_{ax}) in the carbocycle always resonate at lower frequencies than their equatorial counterparts (H_{eq}) and display wider, better-resolved multiplet patterns as a result of large vicinal $J_{Hax,Hax}$ coupling constants. Likewise, the *J* coupling between 4-H_{ax} and 4a-H is larger than that between 4-H_{eq} and 4a-H (10.5–11.5 and 3.7–4.9 Hz, respectively). For compounds in which the heteroring prefers a chair conformation (Figure 1), 4-H_{eq} can also be readily assigned because of its large *J* coupling to the phosphorus atom. Even though the carbocyclic H_{ax} signals did not overlap with the H_{eq} signals, there was often significant overlap amongst the protons in similar stereopositions (e.g., between 6-H_{ax} and 7-H_{ax}); unless an accurate spin simulation was obtained these were only assigned as a group to the corresponding δ range. The C-6 and C-7 carbon signals of the *trans*-fused derivatives could be assigned based on a

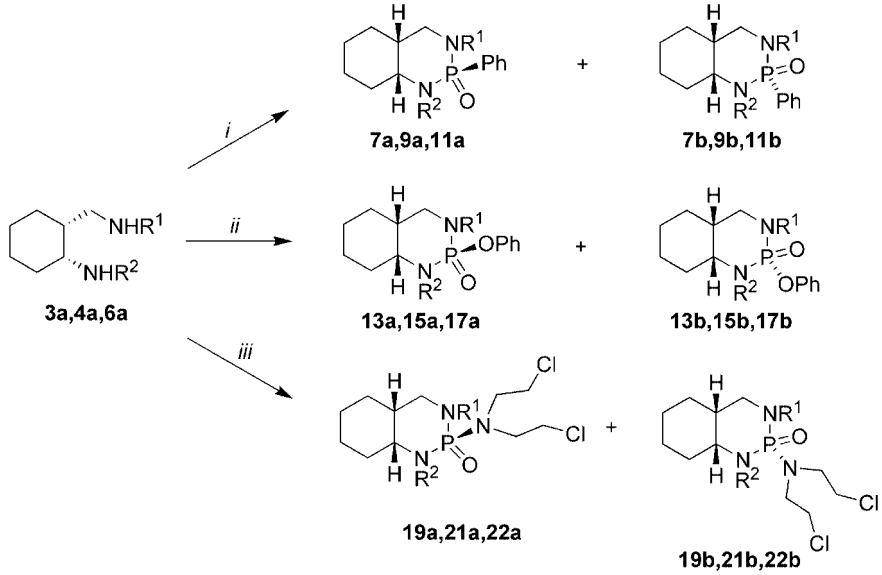

Scheme 2. Reagents and conditions: (*i*) Cl_2POPh/Et_3N, THF, column chromatography, 8–26%; (*ii*) $Cl_2PO(OPh)/Et_3N$, THF, column chromatography, 22–36%; (*iii*) $Cl_2PO[N(CH_2CH_2Cl)_2]/Et_3N$, THF, column chromatography, 15–29%. R^1 = R^2 = H: **3a**, **7**, **13**, **19**; R^1 = Me, R^2 = H: **4a**, **9**, **15**, **21**; R^1 = H, R^2 = Me: **6a**, **11**, **17**, **22**.

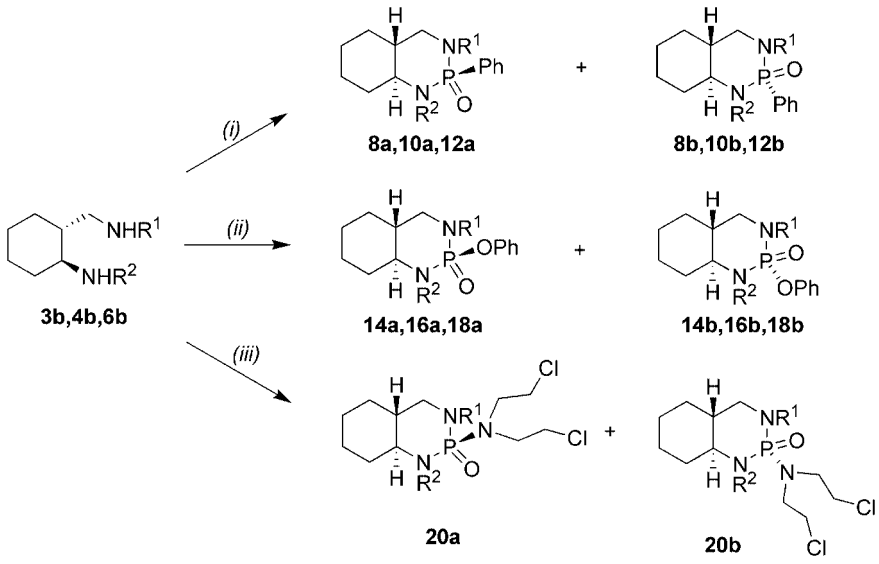

Scheme 3. Reagents and conditions: (*i*) Cl_2POPh/Et_3N, THF, column chromatography, 10–21%; (*ii*) $Cl_2PO(OPh)/Et_3N$, THF, column chromatography, 15–33%; (*iii*) $Cl_2PO[N(CH_2CH_2Cl)_2]/Et_3N$, THF, column chromatography. $R^1 = R^2 =$ H: **3b**, **8**, **14**, **20**; R^1 = Me, R^2 = H: **4b**, **10**, **16**; R^1 = H, R^2 = Me: **6b**, **12**, **18**.

W-type coupling (1.2–3.3 Hz) of the latter to the phosphorus atom, resolved in the 1D ^{13}C NMR spectrum, even when the small difference in their chemical shifts made the assignment by 2D methods uncertain. The compounds in the *cis*-fused series can undergo ring-inversion, which is fast enough on the NMR timescale at 25 °C to yield population-averaged signals. Since the axial and equatorial positions of ring substituents are exchanged upon ring-inversion, we have instead denoted the diastereotopic hydrogen atoms in the *cis* series as H_x and H_y: H_x atoms are axial in the limiting *N-in* invertomer and become equatorial in the *N-out* form (Figure 2) and vice versa for H_y. In the cases in which one of the ring-inverted forms was strongly preferred over the other, the H_x and H_y protons could be readily assigned on the basis of their *J*-coupling patterns in the same way as with the *trans*-fused compounds. For compounds notably populating both forms, a successful spin simulation and a more careful examination of the resulting vicinal coupling constants were required. Also, interpolating the NMR parameters of readily assigned compounds **13a** (assumed to be pure *N-in*, vide infra) and **17b** (assumed to be pure *N-out*) to different population-weighted average values was helpful in the assignment of the carbocyclic part of the *cis* derivatives (the "population" could be varied until the interpolated NMR parameters were consistent with the observed ones).

For each product, the NMR spectra were consistent with the constitution, connectivity and the type of ring-fusion (*cis* or *trans*) of the expected structure. For example, *trans*- and *cis*-fused compounds displayed large (9.4–10.7 Hz) and small (2.7–5.0 Hz) values of $^3J_{4a-H,8a-H}$, respectively, and only in the former series was the W-type $^4J_{P,C-7}$ coupling (1.2–3.3 Hz) resolved; the *ipso*-carbon atom of the aromatic ring in the 2-phenoxy-substituted compounds was deshielded with respect to that of phenyl-substituted compounds (151.4–152.4 and 131.9–134.7 ppm, respectively) and the C-

Table 1. Selected ^1H NMR chemical shifts [ppm] and $J_{H,H}$ and $J_{P,H}$ coupling constants [Hz] for the *trans*-fused compounds at 25 °C in $CDCl_3$ (δ_{TMS} = 0.00 ppm).

	1-R^2	3-R^1	2-Z	4_{ax}[a]	4_{eq}	4a	8a	4_{ax},4_{eq}[b]	4_{ax},4a	4_{ax},P	4_{eq},4a	4_{eq},P	4a,8a	8a,P
8a	H	H	Ph	3.16	3.15	1.61	3.20	–11.3	11.2	3.9	4.4	21.5	10.0	2.1
8b	H	H	Ph	2.73	3.18	1.55	2.70	–12.9	11.0	2.6	3.9	23.8	10.1	–0.6
10a	H	CH_3	Ph	3.05	2.92	1.70	3.16	–11.0	10.8	3.1	4.6	20.2	9.4	2.1
10b	H	CH_3	Ph	2.94	3.05	1.83	2.89	–11.7	11.2	2.8	4.7	16.9	10.1	1.0
12a	CH_3	H	Ph	3.18	3.01	1.71	2.97	–11.7	11.3	3.2	3.6	23.5	10.1	1.9
12b	CH_3	H	Ph	2.93	3.08	1.85	2.90	–13.2	11.1	1.5	3.8	24.2	10.1	1.5
14a	H	H	OPh	2.91	3.16	1.59	2.98	–10.8	11.1	10.6	4.9	11.3	10.3	3.9
14b	H	H	OPh	2.95	3.10	1.44	2.96	–12.9	11.3	1.3	4.0	28.1	10.0	1.3
16a	H	CH_3	OPh	2.85	2.94	1.67	2.98	–10.6	10.5	9.8	4.9	9.4	10.1	3.6
16b	H	CH_3	OPh	2.92	2.90	1.57	2.86	–11.7	11.2	1.4	4.3	26.2	10.1	1.1
18a	CH_3	H	OPh	3.00	3.08	1.97	2.68	–10.9	11.5	5.0	3.7	16.6	10.6	7.2
18b	CH_3	H	OPh	2.91	2.98	1.58	2.82	–13.8	11.5	1.3	4.0	28.2	9.9	1.1
20a	H	H	NR_2[c]	3.08	3.07	1.43	3.07	–11.4	11.4	2.7	4.1	26.1	10.7	0.6
20b	H	H	NR_2[c]	2.78	3.12	1.37	2.74	–13.0	11.1	3.8	4.3	21.3	10.0	0.9

[a] $\delta_{4\text{-Hax}}$ abbreviated to 4_{ax} and similarly for others. [b] $^2J_{4\text{-Hax},4\text{-Heq}}$ abbreviated to 4_{ax},4_{eq} and similarly for others. [c] R = CH_2CH_2Cl.

Table 2. Selected ^{1}H NMR chemical shifts [ppm] for the *cis*-fused compounds at 25 °C in $CDCl_3$ (δ_{TMS} = 0.00 ppm).

	1-R^2	3-R^1	2-Z	4-H_x	4-H_y	4a-H	5-H_x	5-H_y	6-H_x	6-H_y	7-H_x	7-H_y	8-H_x	8-H_y	8a-H
7a	H	H	Ph	3.15	3.12	1.52	2.10	1.37	1.31	1.76	1.63	1.47	1.62	1.73	3.45
7b	H	H	Ph	3.57	3.06	1.87	2.01	1.45	1.37	1.72	1.61	1.43	1.68	1.63	3.86
9a	H	CH_3	Ph	3.27	3.05	1.89	2.13	1.47	1.34	1.70	1.65	1.42	1.65	1.74	3.61
9b	H	CH_3	Ph	3.47	2.83	1.87	2.10	1.48	1.35	1.78	1.54	1.43	1.65	1.65	3.85
11a	CH_3	H	Ph	3.09	3.55	2.30	1.83	1.58	1.47	1.46	1.79	1.27	2.00	1.78	3.11
11b	CH_3	H	Ph	3.25	3.34	2.39	1.82	1.54	1.46	1.44	1.69	1.29	1.80	1.66	3.22
13a	H	H	OPh	3.40	3.01	1.52	2.00	1.32	1.32	1.80	1.55	1.48	1.64	1.65	3.71
13b	H	H	OPh	3.03	3.49	2.18	1.67	1.53	1.42	1.27	1.73	1.26	1.70	1.96	3.41
15a	H	CH_3	OPh	3.35	2.78	1.62	2.01	1.39	1.28	1.76	1.40	1.49	1.58	1.68	3.64
15b	H	CH_3	OPh	2.85	3.43	2.32	1.63	1.52	1.41	1.31	1.72	1.22	1.63	1.87	3.28
17a	CH_3	H	OPh	3.24	2.98	1.77	1.98	1.35	1.38	1.70	1.54	1.39	1.48	2.01	3.30
17b	CH_3	H	OPh	2.88	3.51	2.23	1.63	1.55	1.46	1.22	1.82	1.19	2.04	1.71	3.06
19a	H	H	NR_2	3.20	3.07	1.54	1.85	1.37	1.33	1.71	1.48	1.48	1.65	1.72	3.44
19b	H	H	NR_2	3.49	2.99	1.70	1.85	1.40	1.33	1.73	1.56	1.44	1.64	1.59	3.77
21a	H	CH_3	NR_2	3.03	3.15	1.99	[a]	[b]	[c]	[b]	1.61	[c]	[a]	[a]	3.36[d]
21b	H	CH_3	NR_2	3.34	2.73	1.68	1.83	1.41	1.30	1.77	1.52	1.46	1.60	1.60	3.77
22a	CH_3	H	NR_2	2.94	3.63	2.23	1.66	1.56	1.45	1.31	1.81	1.19	2.09	1.60	2.97
22b	CH_3	H	NR_2	3.26	3.18	2.19	1.75	1.49	1.42	1.49	1.61	1.33	1.69	1.72	3.14

[a] δ = 1.67–1.81 ppm (3 H; 5-H_x, 8-H_x, 8-H_y). [b] δ = 1.45–1.54 ppm (2 H; 5-H_y, 6-H_y). [c] δ = 1.30–1.39 ppm (2 H; 6-H_x, 7-H_y). [d] Under the signals from R = CH_2CH_2Cl, detected by HSQC.

Table 3. ^{13}C NMR chemical shifts [ppm] for the *trans*-fused compounds at 25 °C in $CDCl_3$ (δ_{TMS} = 0.0 ppm).

	1-R^2	3-R^1	2-Z	4	4a	5	6	7	8	8a	R^2	R^1	*i*-C	*o*-C	*m*-C	*p*-C
8a	H	H	Ph	47.0	41.7	28.7	25.4	24.5	35.2	55.5	–	–	134.2	132.3	128.1	131.4
8b	H	H	Ph	48.3	43.1	28.3	25.3	24.8	34.8	57.4	–	–	133.9	131.0	128.5	131.3
10a	H	CH_3	Ph	56.0	42.2	28.7	25.3	24.6	34.7	54.7	–	35.3	132.5	132.8	128.2	131.5
10b	H	CH_3	Ph	57.6	42.1	28.7	25.1	24.7	34.5	56.9	–	35.3	134.5	130.9	128.4	131.0
12a	CH_3	H	Ph	46.1	43.0	29.5	25.3	24.9	30.7	62.5	30.9	–	133.9	132.3	128.2	131.3
12b	CH_3	H	Ph	47.5	42.7	29.1	25.1	25.0	30.8	64.3	30.5	–	134.5	130.9	128.5	131.0
14a	H	H	OPh	47.6	39.9	29.2	25.2	24.2	35.2	56.5	–	–	151.7	121.1	129.4	124.2
14b	H	H	OPh	48.4	42.6	28.0	25.3	24.6	34.5	57.7	–	–	151.4	120.4	129.6	124.3
16a	H	CH_3	OPh	56.4	40.0	29.2	25.0	24.1	35.1	56.6	–	34.9	151.8	121.1	129.4	124.2
16b	H	CH_3	OPh	57.5	42.4	28.3	25.1	24.9	33.8	57.1	–	35.5	151.7	120.4	129.5	124.1
18a	CH_3	H	OPh	47.4	40.4	29.9	25.3	24.5	30.7	64.8	32.0	–	151.8	120.7	129.4	124.0
18b	CH_3	H	OPh	47.4	42.8	28.7	25.0	24.8	30.1	63.6	30.3	–	151.7	120.4	129.5	124.2
20a	H	H	NR_2	47.9	41.3	28.2	25.3	24.3	35.2	56.4	–	–	48.3[a]	42.8[b]	–	–
20b	H	H	NR_2	48.3	43.1	28.5	25.3	24.9	34.6	57.3	–	–	48.7[a]	42.4[b]	–	–

[a] $N(CH_2CH_2Cl)_2$. [b] $N(CH_2CH_2Cl)_2$.

Table 4. ^{13}C NMR chemical shifts [ppm] for the *cis*-fused compounds at 25 °C in $CDCl_3$ (δ_{TMS} = 0.0 ppm).

	1-R^2	3-R^1	2-Z	4	4a	5	6	7	8	8a	R^2	R^1	*i*-C	*o*-C	*m*-C	*p*-C
7a	H	H	Ph	47.0	36.1	24.1	25.1	19.7	32.9	52.1	–	–	133.9	131.0	128.5	131.2
7b	H	H	Ph	45.4	36.0	25.4	24.8	20.4	33.3	50.3	–	–	133.6	132.2	128.2	131.7
9a	H	CH_3	Ph	55.5	36.7	25.6	24.5	20.4	32.5	52.3	–	35.5	134.7	131.1	128.3	130.9
9b	H	CH_3	Ph	55.2	36.6	25.5	25.3	19.8	32.8	49.2	–	35.8	131.9	132.9	128.2	131.7
11a	CH_3	H	Ph	42.3	36.1	28.2	21.8	24.0	27.3	61.4	32.7	–	134.6	132.0	128.2	130.9
11b	CH_3	H	Ph	42.7	36.7	28.0	22.4	23.5	27.2	60.1	33.0	–	134.4	131.9	128.3	131.1
13a	H	H	OPh	47.8	35.7	23.3	25.5	19.1	32.7	52.2	–	–	151.4	120.4	129.6	124.3
13b	H	H	OPh	42.9	36.0	28.3	21.5	24.6	30.7	54.3	–	–	151.6	120.5	129.5	124.2
15a	H	CH_3	OPh	56.9	36.9	24.2	25.4	19.2	31.5	51.8	–	35.6	151.7	120.4	129.5	124.1
15b	H	CH_3	OPh	52.1	35.5	28.3	21.3	24.9	29.9	54.1	–	35.4	152.0	120.4	129.4	123.9
17a	CH_3	H	OPh	45.7	37.1	25.0	24.6	20.2	28.3	59.1	30.7	–	151.9	120.5	129.4	124.0
17b	CH_3	H	OPh	42.2	37.3	29.0	21.2	25.4	24.4	62.6	33.2	–	151.9	120.6	129.4	124.0
19a	H	H	NR_2	46.7	35.5	24.3	24.7	20.2	32.1	52.3	–	–	48.6[a]	42.4[b]	–	–
19b	H	H	NR_2	46.6	35.5	25.0[c]	25.0[c]	20.0	33.3	51.2	–	–	48.3[a]	42.9[b]	–	–
21a	H	CH_3	NR_2	53.5	35.8	26.8	22.9	22.3	31.9	53.3	–	35.4	49.4[a]	42.7[b]	–	–
21b	H	CH_3	NR_2	56.3	36.2	25.3	25.5	19.5	32.9	50.6	–	35.0	49.5[a]	43.0[b]	–	–
22a	CH_3	H	NR_2	41.9	35.6	28.8	21.1	25.2	26.0	62.5	32.4	–	49.8[a]	43.0[b]	–	–
22b	CH_3	H	NR_2	43.7	35.9	27.3	22.6	22.9	27.7	60.4	32.3	–	49.5[a]	42.9[b]	–	–

[a] $N(CH_2CH_2Cl)_2$. [b] $N(CH_2CH_2Cl)_2$. [c] Two adjacent signals at δ = 25.03 and 25.05 ppm; individual assignment not obtained.

Table 5. ^{31}P NMR chemical shifts [ppm] and $J_{P,C}$ coupling constants [Hz] for the *trans*-fused compounds at 25 °C in $CDCl_3$ [δ_P(85% H_3PO_4) = 0.0 ppm].

	δ_P	P,4	P,4a	P,7	P,8	P,8a	P,R^2	P,R^1	P,*i*-C	P,*o*-C	P,*m*-C	P,*p*-C
8a	16.0	4.6	3.1	2.6	9.9	4.2	–	–	163.6	9.8	13.8	3.0
8b	18.7	2.8	6.4	2.7	9.3	2.7	–	–	152.2	10.3	13.7	3.0
10a	19.6	[a]	1.7	1.9	10.1	4.1	–	3.6	163.1	9.7	13.8	2.9
10b	16.3	[a]	5.0	2.2	9.2	3.2	–	4.0	151.2	9.8	13.3	2.8
12a	20.4	3.9	3.6	1.2	6.1	1.5	3.4	–	164.6	9.6	13.7	2.9
12b	18.0	2.8	6.0	1.4	4.9	[a]	4.3	–	150.5	9.6	13.3	3.0
14a	7.2	2.0	11.2	2.7	6.7	1.7	–	–	8.0	4.5	1.2	1.5
14b	8.0	3.7	4.7	3.3	11.4	3.7	–	–	7.9	4.7	0.8	1.0
16a	8.3	2.2	9.2	2.8	7.3	1.8	–	2.9	8.7	4.4	[a]	1.3
16b	9.5	[a]	3.6	3.2	12.0	3.6	–	[a]	9.1	4.5	0.9	1.4
18a	8.8	1.5	12.2	1.5	2.1	1.9	4.3	–	7.6	4.7	1.1	1.2
18b	10.8	3.4	4.7	2.1	8.8	1.6	[a]	–	9.1	4.6	[a]	1.0
20a	15.6	3.3	2.3	2.8	11.0	3.4	–	–	4.7[b]	[a,c]	–	–
20b	14.3	2.9	8.3	2.8	9.2	3.2	–	–	4.2[b]	2.9[c]	–	–

[a] Not resolved. [b] N(*C*H_2CH_2Cl)$_2$. [c] N(CH_2*C*H_2Cl)$_2$.

Table 6. ^{31}P NMR chemical shifts [ppm] and $J_{P,C}$ coupling constants [Hz] for the *cis*-fused compounds at 25 °C in $CDCl_3$ [δ_P(85% H_3PO_4) = 0.0 ppm].

	δ_P	P,4	P,4a	P,8	P,8a	P,R^2	P,R^1	P,*i*-C	P,*o*-C	P,*m*-C	P,*p*-C
7a	19.0	2.7	5.4	8.2	2.7	–	–	152.8	10.2	13.7	2.7
7b	17.6	4.1	3.4	8.8	4.2	–	–	162.0	9.9	13.8	2.9
9a	16.1	[a]	3.5	7.2	3.5	–	4.1	153.2	9.7	13.7	3.0
9b	21.2	[a]	1.5	9.9	4.1	–	3.1	162.6	9.4	13.6	2.9
11a	15.5	3.4	4.6	1.0	[a]	5.4	–	162.2	10.0	13.8	2.7
11b	16.5	3.2	7.3	2.8	[a]	4.6	–	161.0	9.7	13.8	2.8
13a	8.0	3.2	3.8	11.2	3.4	–	–	7.8	4.8	[a]	[a]
13b	7.0	3.2	6.7	[a]	2.8	–	–	7.8	4.8	[a]	1.0
15a	8.9	[a]	2.8	11.5	3.7	–	[a]	9.2	4.6	[a]	0.9
15b	8.4	[a]	5.5	[a]	3.2	–	[a]	8.6	4.5	[a]	[a]
17a	10.2	1.8	6.0	7.8	[a]	[a]	–	9.2	4.6	[a]	0.9
17b	8.4	3.1	6.3	[a]	[a]	1.9	–	8.7	4.6	[a]	1.6
19a	14.4	2.8	6.2	7.6	3.0	–	–	4.3[b]	2.7[c]	–	–
19b	16.8	2.9	3.1	10.7	3.0	–	–	5.0[b]	[a][c]	–	–
21a	14.5	[a]	4.6	4.9	3.5	–	2.8	4.6[b]	[a][c]	–	–
21b	19.6	[a]	1.7	11.7	2.8	–	< 1	4.6[b]	[a][c]	–	–
22a	14.6	2.7	3.5	[a]	1.0	2.9	–	4.6[b]	[a][c]	–	–
22b	15.8	[a]	7.9	4.4	[a]	2.6	–	4.7[b]	[a][c]	–	–

[a] Not resolved. [b] N(*C*H_2CH_2Cl)$_2$. [c] N(CH_2*C*H_2Cl)$_2$.

Table 7. Selected $J_{H,H}$ and $J_{P,H}$ coupling constants [Hz] for the *cis*-fused compounds at 25 °C in $CDCl_3$.

	4_x,4_y	4_x,P	4_y,4a	4_y,P	4a,5_x	5_x,6_x	5_y,6_y	6_x,7_x	6_y,7_y	7_x,8_x	7_y,8_y	8_x,P	8_y,8a	8a,P
7a	–13.3	4.2	3.2	23.1	11.7	12.2	4.3	12.1	4.0	12.8	3.9	5.7	3.8	2.6
7b	–12.2	7.7	4.3	20.3	10.7	11.3	5.0	11.3	4.6	11.8	5.2	4.6	4.2	4.7
9a	–11.8	6.4	4.5	14.7	10.1	10.9	5.5	10.7	5.2	11.3	5.3	4.9	5.1	5.6
9b	–11.5	4.4	3.2	21.7	11.5	12.2	4.5	12.2	3.6	12.4	4.3	5.0	3.6	4.2
11a	–11.6	16.0	10.2	8.3	5.0	4.5	11.5	5.1	11.2	5.4	11.3	[a]	10.3	14.0
11b	–12.1	12.9	9.4	10.9	5.0	6.1	10.7	5.6	10.2	6.2	10.6	[a]	9.7	8.3
13a	–13.3	1.7	2.2	27.9	12.5	13.3	3.0	13.2	3.5	13.9	2.4	7.6	3.3	1.5
13b	–13.2	25.2	11.0	5.9	3.5	4.3	12.4	4.6	11.5	4.1	11.8	[a]	11.1	21.9
15a	–11.9	2.2	2.4	26.1	12.4	13.1	3.1	12.9	3.4	13.6	2.9	6.9	3.2	1.5
15b	–11.8	22.7	11.0	3.6	3.6	3.9	12.5	4.2	11.9	4.5	11.9	[a]	11.5	22.9
17a	–13.2	2.9	4.3	24.6	10.5	11.0	4.8	11.0	5.1	11.7	5.6	4.2	5.1	3.4
17b	–13.6	28.0	12.3	1.6	2.3	2.6	13.8	3.2	13.3	3.0	13.2	[a]	12.3	22.8
19a	–13.3	6.3	3.7	20.2	11.2	11.4	4.8	12.2	4.0	11.4	5.0	5.8	3.7	4.4
19b	–11.9	5.2	3.5	25.2	11.3	11.9	4.5	11.8	4.4	12.1	4.2	6.1	3.9	3.0
21a	–11.8	14.9	7.6	8.2	7.8	[b]	[b]	[b]	[b]	[b]	[b]	[b]	[b]	13.7[b]
21b	–11.6	2.8	2.6	25.5	11.9	12.6	3.6	12.6	3.4	12.9	3.7	6.6	3.3	2.5
22a	–11.5	24.1	11.7	3.5	2.8	2.9	13.5	3.2	12.9	3.6	12.9	[a]	11.9	20.6
22b	–11.5	8.0	8.2	17.4	6.3	6.9	9.4	6.9	9.1	7.3	9.4	1.5	8.5	6.4

[a] Not resolved. [b] Poor ^1H spin simulation due to the presence of impurities in the sample [the **b** epimer and degradation product(s)].

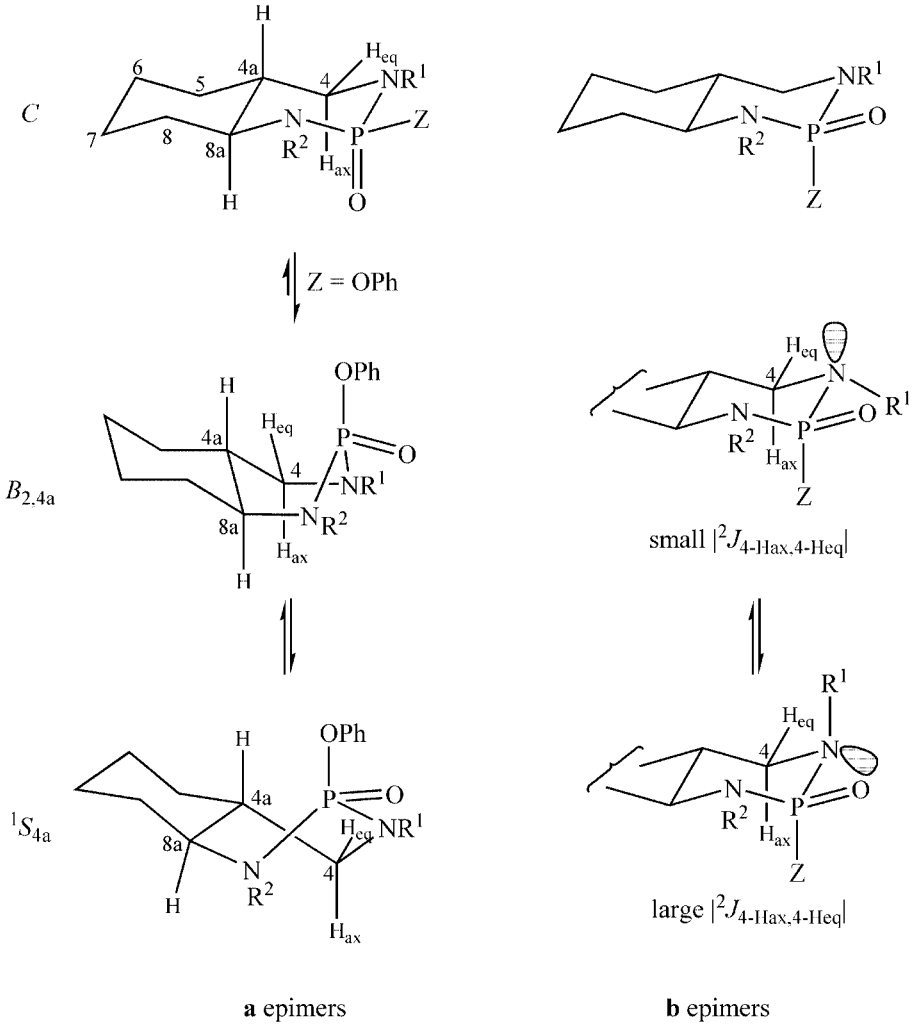

Figure 1. Conformations of the *trans*-fused 1,3,2-diazaphosphinanes. R^1, R^2 = H, CH_3; Z = Ph, OPh, $N(CH_2CH_2Cl)_2$. For both (racemic) epimers, the figure is sketched for the enantiomer with the (4a*R*,8a*S*) configuration.

4 and C-8a carbon atoms were deshielded by around 6–10 ppm upon methyl substitution of the adjacent ring nitrogen atoms (N3 and N1, respectively).

Relative Configurations at Phosphorus

The epimers **a** and **b** differ from each other by the configuration at the phosphorus atom relative to the bridge-head carbons C4a and C8a (Figure 1). The configurations were assigned by NMR methods, the approach depending on the type of ring-fusion (*cis*/*trans*) and the P substituent (Z).

trans-Fused Compounds with Z = Ph (8, 10, 12a,b)

The epimers with an axial Ph substituent (**b**) have smaller $^1J_{P,i\text{-}C}$ values than the equatorial epimers (**a**) (150.5–152.2 and 163.1–164.6 Hz, respectively, Table 5), a trend that has been reported in the literature, for example, for P–C and P–N bonds.[17] Epimers **b**, but not **a**, also display NOESY cross peaks at (*o*-H,4-H_{ax}) and (*o*-H,8a-H) confirming the 1,3-*syn* diaxial nature of 4-H_{ax}, 8a-H and Ph. Consistently with this, in epimers **a** the protons 4-H_{ax} and 8a-H resonate at higher frequencies than those in epimers **b** as a result of the deshielding effect of the 1,3-*syn* diaxial P=O bond.[18,19] On the other hand, the P configurations are not directly evident from the relative phosphorus chemical shifts (Table 5) within an epimeric pair.

trans-Fused Compounds with Z = OPh (14,16,18a,b)

Owing to the well-known axial preference of P–OR and P–OAr bonds in saturated 1,3,2-diheterophosphinane 2-oxides,[13,17] often attributed to the (generalized) anomeric effect, epimers **a** are expected to populate nonchair heteroring conformations with a pseudoaxial phenoxy group whereas epimers **b** should retain a double-chair conformation. The epimers **b** thus have larger $^3J_{P,4\text{-Heq}}$ values than epimers **a** (26.2–28.2 and 9.4–16.6 Hz, respectively, Table 1) since in the former the P2–N3–C4–H_{eq} torsion angle is close to 180° which results in a maximal value of the corresponding coupling constant as per the well-known Karplus relationships.[17] In the **a** series, the 1,4-*syn* axial arrangement of 4a-H and *P*-OPh in the nonchair conformations (Figure 1) results in deshielding of 4a-H and shielding of C-4a with respect to series **b** (Table 1 and Table 3).

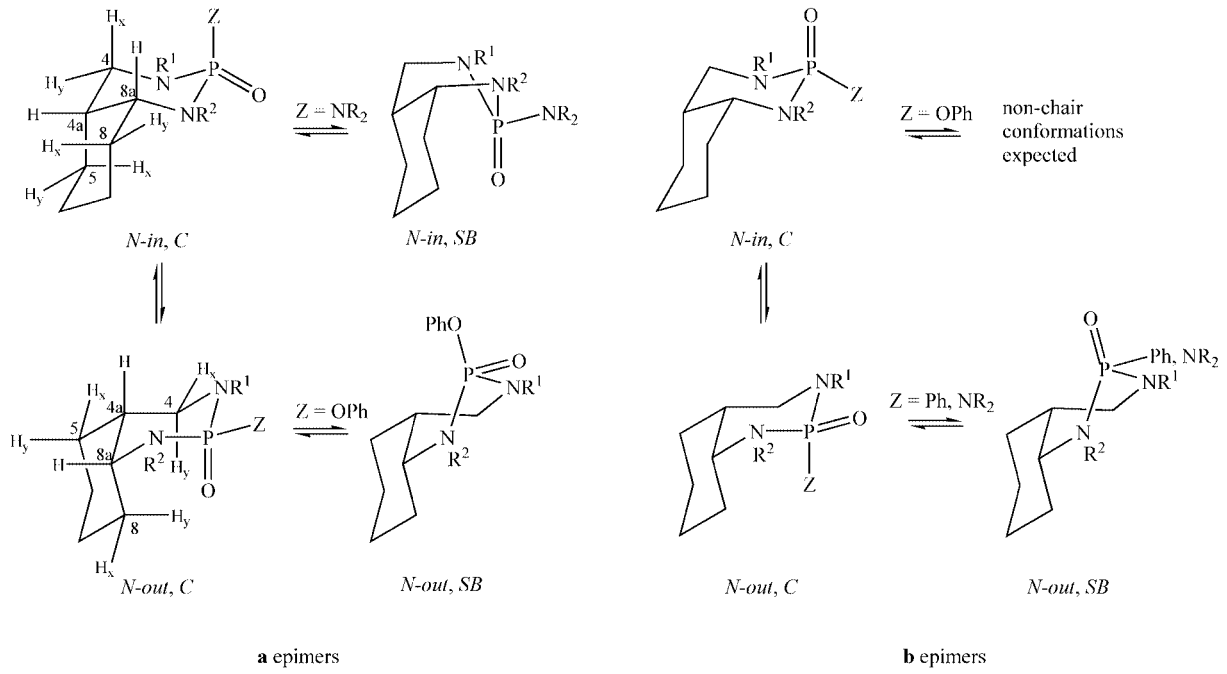

Figure 2. Conformations of the *cis*-fused 1,3,2-diazaphosphinanes. R^1, R^2 = H, CH_3; Z = Ph, OPh, $N(CH_2CH_2Cl)_2$; R = CH_2CH_2Cl. For both (racemic) epimers, the figure is sketched for the enantiomer with the (4a*R*,8a*R*) configuration. *C*: chair heteroring; *SB*: (unspecified) skew-boat heteroring. The *SB* conformations shown are chosen for representative purposes only.

trans-Fused Compounds with Z = N(CH$_2$CH$_2$Cl)$_2$ (20a,b)

The axial P=O, equatorial P–N_{exo} configuration of **20a** may be inferred from the observations that the 4-H_{ax} and 8a-H signals of **20a** are deshielded by around 0.3 ppm with respect to those of **20b** (Table 1) as a result of the deshielding effect[18,19] of an axial P=O bond and that the $|^1J_{P,N\text{-}exo}|$ value of **20a** is larger than that of **20b**, as expected[17] (only for the former epimer was the passive $^1J_{P,N\text{-}exo}$ coupling resolved in the *f*1 dimension of the $^1H\{^{15}N\}$-HMBC spectrum at 20 Hz FID resolution). Also, the selective 1D NOESY spectrum of **20b** showed that the protons 4-H_{ax} and 8a-H are spatially close to the $N(CH_2CH_2Cl)_2$ protons. Similar NOEs were not observed for **20a**.

cis-Fused Compounds

In order to determine the relative P configuration in *cis*-fused compounds, it was necessary to know the position of the *N-in*/*N-out* conformational equilibrium (cf. Figure 2). Fortunately, this could be determined independently (vide infra, Table 8). With the knowledge of the dominant conformation it was then possible to deduce the relative P configuration from NMR criteria similar to those used for *trans*-fused compounds. Thus **7a** and **9a** (Z = Ph, mostly *N-in*) display an NOESY cross-peak at (*o*-H,8a-H) and have a characteristic "axial" $^1J_{P,i\text{-}C}$ value (152.8 and 153.2 Hz, respectively, Table 6), whilst **7b** and **9b** (mostly *N-in* as well) have "equatorial" values of $^1J_{P,i\text{-}C}$ (162.0 and 162.6 Hz, respectively) and have deshielded 4-H_x and 8a-H resonances due to a 1,3-*syn* diaxial P=O. Compounds **11a** and **11b** (Z = Ph) are mostly *N-out*; the *cis* relationship of Ph and 4a-H in **11a** is evident from the observed NOE between 4a-H and the *ortho*-protons of Ph (which is possible if the predominant rotameric state of the phenyl group is similar to that of conformation **A** of **10a** as depicted in Figure 3). Such an NOE was not seen for **11b**. Also, the axial P=O bond in the *N-out* form of **11a** results in a slight deshielding of the 4-H_y proton of epimer **a** with respect to that of **b**. Compounds **13a**, **15a** and **17a** (Z = OPh) have much larger populations of the *N-in* conformation than the corresponding **b** epimers (Table 8) as a result of the axial tendency of OPh.[13,17] On the other hand, compounds **21a** and **22a** [Z = $N(CH_2CH_2Cl)_2$] have larger *N-out* populations than the corresponding **b** epimers since the steric demands of an $N(CH_2CH_2Cl)_2$ substituent outweigh the stereoelectronic ones, driving the substituent towards an equatorial position.[12] Both **19a** and **19b** are predominantly *N-in*, the *N-in* populations being equal within experimental error (85 ± 7 and 87 ± 3%, respectively). The P configuration of these compounds was verified by selective 1D NOESY measurements [in the case of **19a**, 8a-H and $N(CH_2CH_2Cl)_2$ protons received a NOE from 4-H_x] and by the fact that **19b** has deshielded 4-H_x and 8a-H resonances in comparison to those of **19a** (Table 2) due to its 1,3-*syn* diaxial P=O.

Conformations

The conformational processes present in the compounds studied were observed to be fast on the NMR timescale at 25 °C in $CDCl_3$. Thus, only population-weighted averages of the ^1H, ^{13}C and ^{31}P NMR signals were observed. The feasible conformations arise from nitrogen-inversion, P-substituent rotamerism and the different conformational states of the heteroring (e.g., chair or skew-boat). Additionally, in the case of the *cis*-fused compounds simultaneous ring-inversion of both rings resulting in an exchange be-

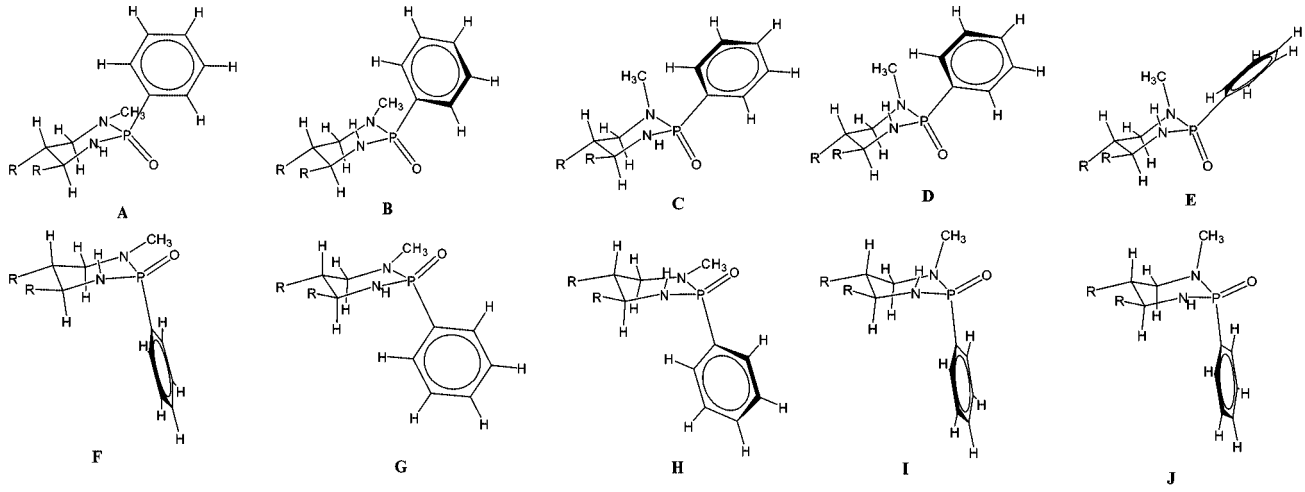

	10a (A-E)					10b (F-J)				
	A	B	C	D	E	F	G	H	I	J
ΔG/ kJ mol^{-1}	0.0[a]	5.0	19.3	38.0	39.8	0.0[b]	0.0	0.5	1.3	2.5
τ(P-N3-C4-H$_{eq}$)/ °	175.3	174.0	–174.6	–177.1	–177.6	168.8	165.2	158.4	176.7	179.3
$^3J_{P,4\text{-Heq}}$/ Hz	23.5	22.1	19.0	17.0	17.0	18.1	18.7	14.8	20.6	23.4
$^2J_{4\text{-Hax},4\text{-Heq}}$/ Hz	–9.9				–13.2		–10.6			–13.6

[a] Reference value for **10a**. [b] Reference value for **10b**.

Figure 3. The optimized chair-like heteroring conformations for **10a** and **10b** and their relative Gibbs energies, P,4-H$_{eq}$ torsion angles and Fermi contact coupling constants $^3J_{P,4\text{-Heq}}$ and $^2J_{4\text{-Hax},4\text{-Heq}}$, as obtained from DFT calculations. –R,R– = –(CH$_2$)$_4$–.

tween the *N-in* and *N-out* forms is a prominent conformational process (Figure 2). In the following, the carbocyclic part is always assumed to adopt a chair conformation. This assumption is confirmed for the *trans*-fused compounds by the expected values of the vicinal $J_{H,H}$ coupling constants in the carbocycle (characteristic "diequatorial" and "diaxial" values) whenever these values could be extracted as well as for the *cis*-fused compounds which notably populate only one of the ring-inverted forms.

trans-Fused Compounds with Z = Ph

From the results for analogous saturated 3,1,2-benzoxazaphosphinine 2-oxides,[13] we expect that the steric requirements of an axial *P*-phenyl substituent in *trans*-fused derivatives are not strong enough to drive the heteroring into nonchair conformations in appreciable amounts. Thus both **a** and **b** epimers of compounds **8**, **10** and **12** are assumed to predominantly populate chair heteroring conformations. Consistently with this, these derivatives generally show large $^3J_{4\text{-Hax},4a\text{-H}}$, $^3J_{P,4\text{-Heq}}$ and $^3J_{P,C\text{-}8}$ and small $^3J_{P,4\text{-Hax}}$ values (Table 1 and Table 5) as expected for double-chair conformations from Karplus-like dependencies of ^3J on the relevant torsion angle. As already noted, the $^1J_{P,i\text{-}C}$ values (Table 5) clearly indicate that the phenyl substituent is equatorial in the case of epimers **a** and axial in the case of epimers **b**, which is also in agreement with a predominant chair heteroring conformation. The $^3J_{P,4\text{-Heq}}$ value for compound **10b** (R^1 = CH$_3$) is surprisingly small (16.9 Hz) in comparison to that of the other compounds in this subset (20.2–24.2 Hz). Based on the DFT coupling-constant calculations on the optimized chair heteroring conformations of **10a** and **10b** (vide infra), such a difference can, however, be fully ascribed to the N^3-methyl substituent effect without taking nonchair conformations into consideration. Similarly, compounds **12a** and **12b** (R^2 = CH$_3$) clearly exhibit smaller values of $^3J_{P,C\text{-}8}$ (6.1 and 4.9 Hz, respectively) than **8**,**10a**,**b** (9.2–10.1 Hz, R^2 = H) due to *N*-methyl substitution in the corresponding coupling pathway. The chair heteroring conformation for **12a**,**b** is nevertheless evident from the other relevant ^3J values.

The substituents at N1 and N3 can be either equatorial or axial and the positions are interconvertible through nitrogen inversion. It is known that the absolute value of a geminal $^2J_{HCH}$ coupling constant decreases when one of the C–H bonds is placed antiperiplanar to an electron lone pair on a directly bonded heteroatom.[20] For the *trans*-fused *P*-phenyl-substituted compounds, the observed $^2J_{4\text{-Hax},4\text{-Heq}}$ values (Table 1) range between –11.0 Hz for **10a** (R^1 = CH$_3$) and –13.2 Hz for **12b** (R^1 = H) which indicates that in the former the N3 substituent is mostly equatorial and in the latter axial (Figure 1 and Figure 3). In general, these values indicate that the N3 substituent in *trans*-fused compounds with an equatorial P=O bond (**b**) adopt an axial position more readily than the other epimer (**a**). When R^1 is hydrogen, its position is clearly axial in **b** and equatorial in **a**, whereas the position of an N^3-methyl group is mostly equatorial also in **b**, as expected from the larger steric size of the methyl group.

DFT Computations for Epimers 10a and 10b

In order to gain more insight into the conformational behavior of *trans*-fused *P*-Ph-substituted compounds and how this behavior is reflected in the NMR parameters, DFT

computations on the P epimeric pair **10a** and **10b** were performed as follows. In the limited conformational search only chair conformations of both rings were considered. As the starting point, the previously optimized double-chair conformations of 3-oxa-analogues (compounds **8a** and **8b** in ref.[13]) were used. The O3 atom was replaced by N–CH_3, and all the possible combinations of axial and equatorial N1 and N3 substituents with two alignments for the phenyl ring [τ(O,P,*i*-C,*o*-C) = 0 or 90°] were constructed, yielding a total of 2×2×2 = 8 starting structures for both **10a** and **10b**. These structures were then subjected to geometry optimization at the B3LYP level of theory using a locally dense basis set (cf. Exp. Sect.) which resulted in five unique optimized geometries for both epimers (Figure 3, **10aA**–**E**, **10bF**–**J**). The subsequent vibrational analyses showed that each of these structures corresponds to a true local minimum in electronic energy. The coupling constants $^3J_{P,4\text{-Heq}}$, $^3J_{P,4\text{-Hax}}$ and in some cases also $^2J_{4\text{-Hax},4\text{-Heq}}$ were then computed at the spin-unrestricted UB3LYP/cc-pVTZ level of theory by the FPT method (cf. Exp. Sect.). Some of the results are summarized in Figure 3 and the Cartesian coordinates and energies of the optimized geometries are provided in the Supporting information.

The calculated relative free energies for the different conformations of **10a** suggest that, in this case, the equatorial position of the N^3-methyl group is much more favorable than the axial one. The axial methyl substituent is likely to interact sterically with the hydrogen atom at C4a and also forces the phenyl ring to assume a sterically more-hindered rotameric state (possibly with reduced conjugation with the P=O bond). On the other hand, both N^3-methyl stereopositions in **10b** are of comparable energy. For this epimer, a destabilizing *gauche* interaction between the methyl and phenyl substituents is removed when the N^3-methyl changes from an equatorial to an axial position. A stabilizing dipole–dipole interaction between the N3–CH_3 and P=O bonds is also possible for both methyl positions in contrast to **10a** in which such an interaction should prefer only the CH_3-equatorial structure. The N3 geometry in the "CH_3-equatorial" structures of **10b** is actually almost planar whereas in those of **10a** it is clearly tetrahedral (the sum of the bond angles is 356.7° for the lowest energy structure of **10b** and 343.2° for that of **10a**). These N3 geometries are likely favored by both the repulsive CH_3/Ph *gauche* interaction and the stabilizing N3–CH_3/P=O dipole–dipole interaction. The near planar N3 geometry in the lowest energy structures of **10b** is concomitant with the flattening of the heteroring and the distortion of the P,4-H_{eq} torsion angle away from the ideal antiperiplanar value. This is reflected in the calculated values of $^3J_{P,4\text{-Heq}}$, as expected from the Karplus relationships, resulting in a population-weighted value of 18.4 Hz for **10b** as opposed to 23.3 Hz for **10a** (at 298.15 K, assuming a Boltzmann distribution). This is in good qualitative agreement with the observed difference in this coupling constant between these epimers (Table 1) and confirms that nonchair conformations need not be considered in order to explain the "small" observed value of $^3J_{P,4\text{-Heq}}$ for **10b**.

The effect of the axial or equatorial position of the CH_3 substituent on the geminal $^2J_{4\text{-Hax},4\text{-Heq}}$ coupling constant was also studied by calculating the Fermi contact contribution to it for representative conformations of **10a** and **10b** (Figure 3). As expected (vide supra), the absolute values in the case of the equatorial CH_3 are smaller (**a**: –9.9 Hz, **b**: –10.6 Hz) than those of the axial CH_3 (**a**: –13.2 Hz, **b**: –13.6 Hz). This, in part, validates the use of $^2J_{4\text{-Hax},4\text{-Heq}}$ as an indicator of the stereoposition of the N3 substituent.

The P–C_{ipso} bond in conformations **F**, **G**, **H** and **J** (Figure 3) is longer than that in **A**–**E** by around 0.01 Å (0.02 Å in the case of **G**). This is as expected for a hyperconjugative n(N) → σ*(P–C) interaction in the former structures in which at least one of the nitrogen lone pairs is antiperiplanar to the P–C bond. The lengthening is in agreement with the smaller observed $^1J_{P,i\text{-C}}$ value for **10b** than for **10a**.

trans-Fused Compounds with Z = OPh

Owing to the favored (pseudo)axial P–OPh, (pseudo) equatorial P=O arrangement of phosphorus substituents (vide supra), the *P*-OPh-substituted epimers **b** are expected to retain chair heteroring conformations. This is readily confirmed, for example, by the large observed $^3J_{P,4\text{-Heq}}$ and $^3J_{P,C\text{-}8}$ and small $^3J_{P,4\text{-Hax}}$ values for **14b**, **16b** and **18b** (Table 1 and Table 5). The *J* values in the corresponding **a** series, in contrast, clearly indicate that the axial preference of OPh forces the heteroring of these epimers to populate nonchair conformations. By taking into consideration the constraints imposed by the *trans*-fused carbocycle and the requirement that OPh be pseudoaxial, as well as the fact that 4-H_{ax} should be *trans*-diaxial with 4a-H in any notably populated conformation (the observed $^3J_{4\text{-Hax},4a\text{-H}}$ values are similar to those of the **b** series), we conclude that the viable boat/skew heteroring conformations in the **a** series are $B_{2,4a}$ and $^1S_{4a}$ (Figure 1). In the $B_{2,4a}$ conformation, the $^3J_{P,4\text{-Hax}}$ and $^3J_{P,4\text{-Heq}}$ values should be nearly equal owing to their comparable torsion angles. This value is estimated to be around 9 Hz from an approximate Karplus-type equation [Eq. (1); parametrized to reproduce the observed $^3J_{P,4\text{-Hax}}$ and $^3J_{P,4\text{-Heq}}$ values for **14b** at τ = (–)60 and 180°]. An inspection of the torsion angles in the idealized $B_{2,4a}$ and $^1S_{4a}$ conformations suggests that the change from $B_{2,4a}$ to $^1S_{4a}$ should be accompanied by an increase in $^3J_{P,4\text{-Heq}}$ and $^3J_{P,8a\text{-H}}$ and a decrease in $^3J_{P,4\text{-Hax}}$ and $^3J_{P,C\text{-}8}$. The observed values of these coupling constants (Table 1 and Table 5) thus show that the predominant heteroring conformation of **14a** and **16a** is close to $B_{2,4a}$, whilst that of **18a** resembles $^1S_{4a}$. In our previous DFT computational and NMR study of 3-oxa-analogues[13] we found a similar shift from $B_{2,4a}$ towards $^1S_{4a}$ conformations upon increasing the steric size of the N1 substituent. The $^3J_{P,4\text{-Hax}}$ and $^3J_{P,4\text{-Heq}}$ values of **18a** (5.0 and 16.6 Hz, respectively) alone could alternatively mean that considerable amounts of a chair conformation is present in this case, but this possibility is excluded by comparison of the values of $^3J_{P,8a\text{-H}}$ and $^3J_{P,C\text{-}8}$ with those of **18b** (which is a double-chair conformation).

$$^3J_{PNCH}\ [\text{Hz}] = 20.5\times\cos^2(\tau) - 7.6\times\cos(\tau) \quad (1)$$

trans-Fused Compounds with Z = N(CH$_2$CH$_2$Cl)$_2$ (20a,b)

The *P*-N(CH$_2$CH$_2$Cl)$_2$ substituent in similar compounds is known to prefer an equatorial position for steric reasons.[12,21] Consistent with this, the heteroring conformation of the epimer **20a** can be readily verified as a chair from the *J*-coupling-constant criteria similar to those used above. As in the **a** series of *P*-phenyl-substituted compounds, its N3 hydrogen atom is predominantly equatorial ($^2J_{4\text{-Hax},4\text{-Heq}}$ = –11.4 Hz). The epimer **20b** is also predominantly in a double-chair conformation, but displays slightly smaller $^3J_{P,4\text{-Heq}}$ and $^3J_{P,C\text{-}8}$ and slightly larger $^3J_{P,4\text{-Hax}}$ values than **20a**. This could indicate a small contribution from nonchair heteroring conformations or simply reflect some distortion of torsion angles in the chair conformation in response to the sterically demanding axial P substituent. In compound **20b** the N3 hydrogen atom preferentially adopts an axial position ($^2J_{4\text{-Hax},4\text{-Heq}}$ = –13.0 Hz), as is generally observed in this study for compounds with an equatorial P=O bond.

cis-Fused Compounds

In the *cis*-fused compounds, interconversion between the *N-in* and *N-out* forms (Figure 2) is possible. The N1 atom is axial with respect to the fused carbocycle in the former, and equatorial in the latter. The observed NMR parameters are population-weighted averages of the parameters of the limiting forms, which can be expressed by Equation (2), where *P* can be, for example, a chemical shift or a *J* coupling constant, or a linear combination thereof, and *x*(*N-in*) and *x*(*N-out*) are the fractional populations of the limiting forms. The parameters *P*(*N-in*) and *P*(*N-out*) can themselves be averages of several heteroring conformations, for example. We will use Equation (2) in two ways. First, we will select a set of NMR parameters P^{I} for which P^{I}(obs) is sensitive (only) to the position of the *N-in*/*N-out* equilibrium and for which both P^{I}(*N-in*) and P^{I}(*N-out*) can be reliably estimated. We will then use these in Equation (2) to yield the fractional population of the *N-in* form for each compound. Secondly, we consider certain parameters P^{II} for which P^{II}(*N-in*) and P^{II}(*N-out*) are sensitive to the heteroring conformation of the corresponding form and calculate the value of P^{II} in one of the limiting forms by estimating the value in the other form.

$$P(\text{obs}) = x(N\text{-}in) \times P(N\text{-}in) + x(N\text{-}out) \times P(N\text{-}out) \quad (2)$$

Position of the N-in/N-out Equilibrium in the cis-Fused Compounds

The *x*(*N-in*) values for the *cis*-fused compounds were calculated from Equation (2) by using the following 10 NMR parameters for P^{I}: $^3J_{\text{Hx,Hx}}$ coupling constants in the carbocycle (three different, cf. Figure 2 and Table 7), $^3J_{\text{Hy,Hy}}$ (three different), $^3J_{4\text{-Hy},4a\text{-H}}$, $^3J_{4a\text{-H},5\text{-Hx}}$, $^3J_{8\text{-Hy},8a\text{-H}}$ and $\delta_{C\text{-}6} - \delta_{C\text{-}7}$ (Table 4). The mean values of the 10 calculations for each compound are given in Table 8. The selected coupling constants are very sensitive to the position of the *N-in*/*N-out* equilibrium as a result of the large change in the dihedral angle between the coupled protons upon ring-inversion, but their values in the limiting *N-in* and *N-out* forms are expected to be insensitive to heteroring substitution and conformation. The ^{13}C chemical-shift difference $\delta_{C\text{-}6} - \delta_{C\text{-}7}$ is positive in *N-in* and negative in *N-out* due to γ-*gauche* shielding[22] of C-7 in *N-in* and C-6 in *N-out*. The values of P^{I}(*N-in*) and P^{I}(*N-out*) were obtained from compounds **13a** and **17b**, respectively. These compounds display extreme values for the parameters P^{I} within the *cis*-fused series and their $^3J_{\text{H,H}}$ values are also similar to the $^3J_{\text{Hax,Hax}}$ and $^3J_{\text{Heq,Heq}}$ values of the *trans*-fused compounds.

The *x*(*N-in*) values (Table 8) obtained demonstrate remarkable effects of the P and N substituents and the P configuration on the *N-in*/*N-out* equilibrium. The substitution of the N1 hydrogen atom by a methyl group is accompanied by a considerable shift towards the *N-out* form when the other substituents and the P configuration are kept constant (e.g., **7a** → **11a**, **7b** → **11b**, **13a** → **17a**). The increase in the steric size of the N1 substituent thus drives the N1 atom into an equatorial position with respect to the fused carbocycle, as previously observed for the 3-oxa-analogues.[13] The effect of P substitution depends both on the type of substituent and the P configuration. The axial preference of a *P*-phenoxy group is evidently the strongest single factor affecting the *N-in*/*N-out* equilibrium within the studied range of N1, P2 and N3 substituents, as seen by the preference of the *N-in* form in the **a** epimers and the *N-out* form in the **b** epimers of compounds **13**, **15** and **17**. Combined with the effect from the N1 substituent, this allows the above use of **13a** and **17b** as model compounds for the *N-in* and *N-out* forms to be rationalized. In contrast, *P*-phenyl and -N(CH$_2$CH$_2$Cl)$_2$ substituents prefer an equatorial position for steric reasons, as already mentioned. Thus, the *N-in* population in the **b** epimers of **9**, **11**, **21** and **22** is larger than in the respective **a** epimers. By comparing the *x*(*N-in*) values within, for example, the **9a**/**21a** or **11a**/**22a** pair [the same N1 and N3 substitution, but the first member has phenyl and the second N(CH$_2$CH$_2$Cl)$_2$ as the P substituent], it is obvious that the phenyl group is sterically less demanding than N(CH$_2$CH$_2$Cl)$_2$ in these compounds. Finally, the effect of the N3 substituent seems to comprise both steric and stereoelectronic factors. When the N3 substituent is hydrogen, the ring-inverted form with an equatorial P=O bond is stabilized as a result of a dipole–dipole interaction (or even an unconventional hydrogen bond) between N–H and P=O. These bonds can become more parallel through an increase in the planarity of the N3 nitrogen atom if P=O is equatorial. Thus, in the **a** series, the replacement of the N^3-methyl by a hydrogen atom (**9a** → **7a**, **21a** → **19a**) results in an increased population of the *N-in* form, but a decreased one in the **b** series (**9b** → **7b**, **21b** → **19b**). Also, compound **7a** (Z = Ph, R^1 = H) displays a larger population of the *N-in* form (0.91) than **7b** (0.82) despite the (weak) equatorial preference of Ph. In the case of *P*-phenoxy substitution, however, an increase in the steric size of the N3 substituent seems to favor the *N-out* form regard-

Table 8. The *N-in*/*N-out* equilibrium for the *cis*-fused compounds at 25 °C in $CDCl_3$. *N-in* mol fractions x(*N-in*) and predominant heteroring conformations (chair or skew-boat) in the limiting forms with some relevant coupling constants [Hz].

	x(*N-in*)[a]	P^{II}(obs)				P^{II}(*N-in*)				P^{II}(*N-out*)		
		$^3J_{P,4\text{-}Hx}$	$^3J_{P,4\text{-}Hy}$	$^1J_{P,C}$	[b]	$^3J_{P,4\text{-}Hx}$	$^3J_{P,4\text{-}Hy}$	$^1J_{P,C}$	[c]	$^3J_{P,4\text{-}Hx}$	$^3J_{P,4\text{-}Hy}$	$^1J_{P,C}$
Z = Ph												
7a	0.91 ± 0.03	4.2	23.1	152.8	*C*	2.5 ± 1.3	25.0 ± 1.4	151.7 ± 1.1	*C**	21.5	3.9	163.6
9a	0.77 ± 0.03	6.4	14.7	153.2	*C*	2.3 ± 1.8	18.1 ± 1.7	150.2 ± 1.6	*C**	20.2	3.1	163.1
11a	0.21 ± 0.03	16.0	8.3	162.2	[d]	[d]	[d]	[d]	*C**	23.5	3.2	164.6
7b	0.82 ± 0.05	7.7	20.3	162.0	*C**	3.9	21.5	163.6	[d]	[d]	[d]	[d]
9b	0.90 ± 0.05	4.4	21.7	162.6	*C**	3.1	20.2	163.1	[d]	[d]	[d]	[d]
11b	0.28 ± 0.03	12.9	10.9	161.0	*C**	3.2	23.5	164.6	*SB*	16.8 ± 1.8	6.0 ± 2.0	159.6 ± 1.5
Z = OPh												
13a[e]	1.00	1.7	27.9	–	*C**	1.3	28.1	–	[f]	[f]	[f]	–
15a	0.99 ± 0.02	2.2	26.1	–	*C**	1.4	26.2	–	[f]	[f]	[f]	–
17a	0.79 ± 0.04	2.9	24.6	–	*C**	1.3	28.2	–	*SB*	8.9 ± 9.5	11.2 ± 11.3	–
13b	0.13 ± 0.03	25.2	5.9	–	[d]	[d]	[d]	–	*C**	28.1	1.3	–
15b	0.11 ± 0.02	22.7	3.6	–	[d]	[d]	[d]	–	*C**	26.2	1.4	–
17b[e]	0.00	28.0	1.6	–	[f]	[f]	[f]	–	*C**	28.2	1.3	–
Z = NR_2												
19a	0.85 ± 0.07	6.3	20.2	–	*C*	2.8 ± 2.8	23.2 ± 2.5	–	*C**	26.1	2.7	–
21a[g]	0.49 ± 0.04	14.9	8.2	–	*SB*	5.2 ± 4.1	13.9 ± 3.5	–	*C**	26.1[h]	2.7[h]	–
22a	0.03 ± 0.02	24.1	3.5	–	[d]	[d]	[d]	–	*C**	26.1	2.7	–
19b	0.87 ± 0.03	5.2	25.2	–	*C**	2.7	26.1	–	[d]	[d]	[d]	–
21b	0.95 ± 0.04	2.8	25.4	–	*C**	2.7[h]	26.1[h]	–	[d]	[d]	[d]	–
22b	0.39 ± 0.02	8.0	17.4	–	*C**	2.7	26.1	–	*SB*	11.4 ± 2.1	11.8 ± 2.3	–

[a] Arithmetic mean ± standard deviation of 10 calculations of x(*N-in*) using Equation (2) with the parameter set P^I (see text). [b] Predominant heteroring conformation in the *N-in* form. *C*: chair, *SB*: skew-boat (unspecified). An asterisk indicates an assumed chair conformation and its P^{II} values are taken from the corresponding *trans* derivative (see text). Values for nonasterisked conformations are derived from Equation (2) [errors are from a total differential; assuming ΔP(obs) ± 0.5 Hz and $\Delta P(C^*)$ ± 1.5 Hz]. [c] Predominant heteroring conformation in the *N-out* form. [d] Uncertain owing to the small population of the corresponding form. [e] Reference compounds for the P^I(*N-in*) and P^I(*N-out*) values in Equation (2). [f] Zero population within experimental error. [g] x(*N-in*) calculated from $J_{4y,4a}$, $J_{4a,5x}$ and ($\delta_{C\text{-}6}$–$\delta_{C\text{-}7}$) only. [h] Values from **20a** are used.

less of the P configuration: in these compounds the axial preference of OPh likely forces the P=O bond to be equatorial in both the *N-in* and *N-out* forms (vide infra).

Heteroring Conformations in the Limiting N-in and N-out Forms

We assume that the heteroring in the limiting forms is chair whenever it results in the adoption of the preferred position for the P substituent [axial for OPh, equatorial for Ph and $N(CH_2CH_2Cl)_2$]. Thus, with the *P*-OPh derivatives, the *N-in* form of the **a** epimers and the *N-out* form of the **b** epimers are expected to adopt a double-chair conformation and vice versa for the "steric" P substituents. This assumption is validated, for example, by the fact that the observed $^3J_{P,4\text{-}Hx}$ and $^3J_{P,4\text{-}Hy}$ values are consistent with a chair structure for compounds in which the assumed double-chair structure is almost exclusively populated (**13a**, **17b** etc.).

To analyse the "nonassumed" heteroring conformations, two to three NMR P^{II} parameters were chosen: $^3J_{P,4\text{-}Hx}$, $^3J_{P,4\text{-}Hy}$ and, for the *P*-phenyl-substituted derivatives, $^1J_{P,i\text{-}C}$. The values for the assumed double-chair structures were obtained from the corresponding *trans*-fused compounds (with similar substitution and stereoposition of the P substituent), from which the values for the other ring-inverted form were calculated using Equation (2). The results are summarised in Table 8. Although this calculation gave unacceptable error limits in cases in which the population of the corresponding form was less than around 20%, some general conclusions can be drawn. The results for the *P*-OPh derivatives are consistent with the assumption that conformations with a (pseudo)axial phenoxy group are almost exclusively populated. That is, the epimers **a** of **13**, **15** and **17** should adopt a double-chair conformation in the *N-in* form and a skew-boat heteroring conformation(s) in the *N-out* form, and vice versa for the epimers **b** (Figure 2). The presence of nonchair conformations could, indeed, be verified for the *N-out* form of **17a** (Table 8), whilst the *N-in*/*N-out* equilibrium of the other phenoxy-substituted derivatives was too strongly biased for the verification of nonchair conformations. Nonchair heteroring conformations for derivatives with a "steric" P substituent (Ph, NR_2) are reasonable only for the *N-in*-**a** and *N-out*-**b** structures. In the former, the steric environment of the P substituent is similar to that of the *trans*-fused **b** epimers (two 1,3-*syn* diaxial hydrogen atoms) and, by analogy, it is no surprise that *N-in*-**7a**, -**9a** and -**19a** are observed to adopt double-chair conformations with an axial P substituent (Table 8, Figure 2). Remarkably, skew-boat conformations seem to contribute to the *N-in*-**21a** form (R^2 = H, R^1 = CH_3, Z = NR_2). This can be explained by the loss of one stabilizing N–H/P=O dipole–dipole interaction in the double-chair conformation in comparison to *N-in*-**19a** (R^1 = R^2 = H). In the *N-out*-**b** structures with a steric P substituent the preference for nonchair conformations should be greater than

that in the *trans*-fused **b** epimers due to the presence of a 1,3-*syn* diaxial methylene group, $C(8)H_2$, in a chair conformation. Consistent with this, a notable contribution from nonchair conformations to *N-out*-**11b** and -**22b** is feasible based on the P^{II}(*N-out*) values in Table 8. For the former, this is most clearly seen from the large $^1J_{P,C}$(*N-out*) value (159.6 Hz) which implies that the P–C bond is predominantly pseudoequatorial.

Conclusions

The preferred conformations of the prepared saturated 1,3,2-benzodiazaphosphinine 2-oxides display a clear dependence on the nature of the N and P substituents and the P configuration. The *P*-phenoxy substituent has a strong stereoelectronic axial preference resulting in population of skew-boat heteroring conformations whenever the axial position cannot be obtained in a chair structure. The *N-in*/*N-out* equilibrium in the *cis*-fused derivatives is also strongly biased towards the form in which a double-chair conformation and an axial position for OPh can be simultaneously attained. The *P*-phenyl and -bis(2-chloroethyl)amino substituents generally display a steric equatorial preference, the latter more so than the former, as is evident from the position of the *N-in*/*N-out* equilibrium in the *cis*-fused derivatives. Nevertheless, the *trans*-fused derivatives studied here retain chair conformations in the case of axial Ph or $N(CH_2CH_2Cl)_2$ substitution. Methyl substitution of the N1 atom in the *cis*-fused series drives the *N-in*/*N-out* equilibrium towards the *N-out* form and in the *trans*-fused *P*-OPh-substituted **a** series it drives the predominant heteroring conformation from $B_{2,4a}$ towards $^1S_{4a}$. A N^3-hydrogen substituent seemingly has a stabilizing effect on conformations with an equatorial P=O bond.

Experimental Section

NMR Spectroscopy: NMR spectra were recorded with JEOL JNM-LA400 and JNM-A500 and Bruker Avance 400 and 500 NMR spectrometers at 25 °C using $CDCl_3$ as solvent. The following NMR spectra were acquired for each compound: ^1H, ^{13}C with ^1H-decoupling , ^{31}P with ^1H-decoupling, dqf-COSY and $^1H\{^{13}C\}$-HSQC or $^{13}C\{^1H\}$-HETCOR. In addition, ^1H NMR with ^{31}P-decoupling, NOE difference, 1D and/or 2D NOESY, $^1H\{^{15}N\}$-HMBC, $^1H\{^{13}C\}$-HMBC and/or $^{13}C\{^1H\}$-COLOC experiments were acquired when deemed necessary. Typical acquisition and processing parameters are provided in the Supporting Information. The ^1H and ^{13}C chemical shifts are referenced to internal tetramethylsilane (δ_{TMS} = 0.00 ppm), and the ^{31}P shifts are referenced to the ^1H resonance of internal TMS according to the unified shift scale[23] recommended by IUPAC (secondary reference 85% H_3PO_4: Ξ_P = 40.480742, δ_P = 0.0 ppm). ^1H chemical shifts and $J_{H,H}$ and $J_{P,H}$ coupling constants were extracted by an iterative analysis of the ^1H NMR spectra using the PERCH NMR software.[24] The initial trial parameters for the iterative analysis were obtained, as far as possible, manually from the ^1H NMR spectra and were complemented by use of "chemical intuition" and results from earlier successful analyses. These trial parameters were refined by using the software in integral-transform-fitting mode (D mode) until a good match with the observed spectrum was obtained, followed by total line-shape fitting (T mode) to yield the reported δ_H, $J_{H,H}$ and $J_{P,H}$ values. RMS errors of the iteratively solved ^1H NMR spectra together with an example of a simulated vs. observed spectrum may be found in the Supporting information.

Computations: Computations were performed with the Gaussian 98 electronic structure program.[25] Geometry optimizations and subsequent vibrational analyses (1 bar, 298.15 K, scaling factor 0.9804) [26] were performed at the B3LYP level of theory[27–29] by using a locally dense basis set: the $-(CH_2)_4-$ part of the molecule was defined by the basis set 3-21G, heteroatoms by 6-31+G(d,p) and all the other atoms by 6-31G(d,p). Thermal free-energy values and the number of imaginary frequencies for each optimized structure were obtained from the vibrational analyses (no imaginary frequencies were found, confirming that the geometries obtained corresponded to energy minima). The Fermi contact (FC) contribution to *J*-coupling constants was calculated by the finite perturbation theory (FPT) method,[30,31] at the spin-unrestricted UB3LYP/cc-pVTZ level, by applying a perturbation of 0.01 au to the phosphorus atom ($^3J_{P,H}$) or to one of the 4-H protons ($^2J_{H,H}$) with the FIELD keyword of Gaussian 98. Other contributions to the *J* coupling constants were omitted in this study. The calculated $J_{P,H}$ coupling constants were scaled by using the calibration equation of Tähtinen et al.[31] (Figure 3 in ref.[31]). Both in the geometry optimizations and the FC calculations, tight SCF convergence criteria were used.

General Procedures: Melting points were recorded on a Kofler hot plate microscope apparatus and are uncorrected. Elemental analyses were performed with a Perkin–Elmer 2400 CHNS elemental analyzer. Mass spectra were recorded on a Finnigan MAT 95S and a ZabSpecETOF instrument using electron-impact ionization. Chemicals were generally of the highest purity. Silica gel 60 (0.040–0.063 mm) was used for column chromatography. Merck Kieselgel $60F_{254}$ plates were used for TLC.

Carboxamides **1a**, **1b**, **2a** and **2b**[15] and the diamines **4a** and **4b**[16] were prepared according to literature procedures.

***cis*- and *trans*-2-(Aminomethyl)cyclohexylamine (3a and 3b):** *cis*- or *trans*-2-Aminocyclohexanecarboxamide (**1a** or **1b**) (7.11 g, 50 mmol), respectively, was added in small portions to a stirred and cooled suspension of $LiAlH_4$ (11.39 g, 300 mmol) in dry THF (400 mL). The mixture was stirred and refluxed for 12 h and then cooled and the excess $LiAlH_4$ was decomposed by the addition of a mixture of water (22.8 mL) and THF (50 mL). The inorganic salts were filtered off and washed with EtOAc (3 × 100 mL). The combined organic filtrate and washings were dried (Na_2SO_4) and evaporated under reduced pressure to give an oily product. The crude diamines were purified by distillation.

3a: Colorless oil; yield: 3.27 g (51%); b.p. 87–88 °C (13 Torr). The ^1H NMR spectroscopic data of the product correspond to the literature[32] data of the enantiomerically pure isomer.

3b: Colorless oil; yield: 3.53 g (55%); b.p. 67–69 °C (14 Torr). The ^1H NMR spectroscopic data of the product correspond to the literature[32] data of the enantiomerically pure isomer.

***cis*-2-(Ethoxycarbonylamino)cyclohexanecarboxamide (5a):** Ethyl chloroformate (6.51 g, 60 mmol) was added to a stirred mixture of carboxamide **1a** (7.11 g, 50 mmol), toluene (150 mL), $NaHCO_3$ (6.30 g, 75 mmol) and H_2O (150 mL) and the mixture was stirred at room temperature for 1 h. The organic layer was separated and the aqueous layer was extracted with EtOAc (3 × 75 mL). The combined extracts were dried (Na_2SO_4) and evaporated to yield a crystalline product.

5a: White crystals; yield: 8.04 g (75%). Compound **5a** was used in the next step without further purification.

***trans*-2-(Ethoxycarbonylamino)cyclohexanecarboxamide (5b):** $NaHCO_3$ (5.04 g, 60 mmol), H_2O (80 mL) and ethyl chloroformate (5.21 g, 48 mmol) were added to a stirred mixture of carboxamide **1b** (5.69 g, 40 mmol) and toluene (80 mL) and the mixture was stirred at room temperature for 1 h. The precipitated white crystals were filtered off and washed with H_2O and Et_2O to yield a crystalline product.

5b: White crystals; yield: 8.40 g (98%). Compound **5b** was used in the next step without further purification.

***cis*- and *trans*-2-(Methylamino)cyclohexylmethylamine (6a and 6b):** The corresponding carboxamide (**5a** or **5b**) (7.93 g, 37 mmol) was added in small portions to a stirred and cooled suspension of $LiAlH_4$ (4.21 g, 111 mmol) in dry THF (200 mL). The mixture was stirred and refluxed for 3 h and then cooled and the excess $LiAlH_4$ was decomposed by the addition of a mixture of water (8.4 mL) and THF (40 mL). The inorganic salts were filtered off and washed with EtOAc (3 × 75 mL). The combined organic filtrate and washings were dried (Na_2SO_4) and evaporated under reduced pressure to give an oily product. The crude diamines were purified by distillation.

6a: Colorless oil; yield: 2.26 g (43%); b.p. 77–78 °C (15 Torr). The ^{1}H NMR spectroscopic data of the product correspond to the literature[33] data.

6b: Colorless oil; yield: 1.89 g (36%); b.p. 70–71 °C (14 Torr). The ^{1}H NMR spectroscopic data of the product correspond to the literature[34] data.

General Method for Ring-Closure Reactions: A solution of the appropriate phosphorus-containing reagent [phenylphosphonic dichloride, phenyl dichlorophosphate or bis(2-chloroethyl)phosphoramidic dichloride, 1 equiv.] in dry THF (50 mL) was added dropwise to a stirred solution of the appropriate diamine (**3a**,**b**, **4a**,**b** and **6a**,**b**, 7 mmol) and triethylamine (2 equiv.) in dry THF (100 mL) at room temperature. The reaction mixture was stirred for 48 h at room temperature and then filtered to remove triethylamine hydrochloride. The filtrate was evaporated to dryness. From the crude product, epimers **a** and **b** were obtained in pure form as described in Table 9. ^{1}H, ^{13}C and ^{31}P NMR spectroscopic data of products **7**–**22a**,**b** are given in Tables 1, 2, 3, 4, 5, 6, and 7 and in the Supporting Information.

***rac*-(2*S*,4a*R*,8a*R*)- and *rac*-(2*R*,4a*R*,8a*R*)-2-Phenyl-1,2,3,4,4a,5,6,7,8,8a-decahydro-1,3,2-benzodiazaphosphinine 2-Oxide (7a and 7b)**

7a: $C_{13}H_{19}N_2OP$ (250.28): calcd. C 62.39, H 7.65, N 11.19; found C 62.07, H 7.36, N 10.82. MS: *m*/*z* = 250 $[M]^+$.

7b: $C_{13}H_{19}N_2OP$ (250.28): calcd. C 62.39, H 7.65, N 11.19; found C 62.12, H 7.74, N 11.32. MS: *m*/*z* = 250 $[M]^+$.

***rac*-(2*S*,4a*R*,8a*S*)- and *rac*-(2*R*,4a*R*,8a*S*)-2-Phenyl-1,2,3,4,4a,5,6,7,8,8a-decahydro-1,3,2-benzodiazaphosphinine 2-Oxide (8a and 8b)**

8a: $C_{13}H_{19}N_2OP$ (250.28): calcd. C 62.39, H 7.65, N 11.19; found C 62.51, H 7.40, N 10.79. MS: *m*/*z* = 250 $[M]^+$.

8b: $C_{13}H_{19}N_2OP$ (250.28): calcd. C 62.39, H 7.65, N 11.19; found C 62.19, H 7.57, N 10.64. MS: *m*/*z* = 250 $[M]^+$.

***rac*-(2*R*,4a*R*,8a*R*)- and *rac*-(2*S*,4a*R*,8a*R*)-3-Methyl-2-phenyl-1,2,3,4,4a,5,6,7,8,8a-decahydro-1,3,2-benzodiazaphosphinine 2-Oxides (9a and 9b)**

9a: $C_{14}H_{21}N_2OP$ (264.30): calcd. C 63.62, H 8.01, N 10.60; found C 64.04, H 7.79, N 10.86. MS: *m*/*z* = 264 $[M]^+$.

9b: $C_{14}H_{21}N_2OP$ (264.30): calcd. C 63.62, H 8.01, N 10.60; found C 63.25, H 8.20, N 10.79. MS: *m*/*z* = 264 $[M]^+$.

***rac*-(2*R*,4a*R*,8a*S*)- and *rac*-(2*S*,4a*R*,8a*S*)-3-Methyl-2-phenyl-1,2,3,4,4a,5,6,7,8,8a-decahydro-1,3,2-benzodiazaphosphinine 2-Oxide (10a and 10b)**

10a: $C_{14}H_{21}N_2OP$ (264.30): calcd. C 63.62, H 8.01, N 10.60; found C 63.98, H 8.20, N 10.97. MS: *m*/*z* = 264 $[M]^+$.

10b: $C_{14}H_{21}N_2OP$ (264.30): calcd. C 63.62, H 8.01, N 10.60; found C 63.89, H 7.83, N 11.01. MS: *m*/*z* = 264 $[M]^+$.

***rac*-(2*S*,4a*R*,8a*R*)- and *rac*-(2*R*,4a*R*,8a*R*)-1-Methyl-2-phenyl-1,2,3,4,4a,5,6,7,8,8a-decahydro-1,3,2-benzodiazaphosphinine 2-Oxides (11a and 11b)**

11a: $C_{14}H_{21}N_2OP$ (264.30): calcd. C 63.62, H 8.01, N 10.60; found C 63.47, H 8.24, N 10.44. MS: *m*/*z* = 264 $[M]^+$.

11b: $C_{14}H_{21}N_2OP$ (264.30): calcd. C 63.62, H 8.01, N 10.60; found C 63.38, H 7.75, N 10.47. MS: *m*/*z* = 264 $[M]^+$.

***rac*-(2*S*,4a*R*,8a*S*)- and *rac*-(2*R*,4a*R*,8a*S*)-1-Methyl-2-phenyl-1,2,3,4,4a,5,6,7,8,8a-decahydro-1,3,2-benzodiazaphosphinine 2-Oxides (12a and 12b)**

12a: $C_{14}H_{21}N_2OP$ (264.30): calcd. C 63.62, H 8.01, N 10.60; found C 63.89, H 8.27, N 10.42. MS: *m*/*z* = 264 $[M]^+$.

12b: $C_{14}H_{21}N_2OP$ (264.30): calcd. C 63.62, H 8.01, N 10.60; found C 63.43, H 7.72, N 11.10. MS: *m*/*z* = 264 $[M]^+$.

***rac*-(2*R*,4a*R*,8a*R*)- and *rac*-(2*S*,4a*R*,8a*R*)-2-Phenoxy-1,2,3,4,4a,5,6,7,8,8a-decahydro-1,3,2-benzodiazaphosphinine 2-Oxides (13a and 13b)**

13a: $C_{13}H_{19}N_2O_2P$ (266.28): calcd. C 58.64, H 7.19, N 10.52; found C 58.50, H 7.38, N 10.23. MS: *m*/*z* = 266 $[M]^+$.

13b: $C_{13}H_{19}N_2O_2P$ (266.28): calcd. C 58.64, H 7.19, N 10.52; found C 58.43, H 6.93, N 10.76. MS: *m*/*z* = 266 $[M]^+$.

***rac*-(2*R*,4a*R*,8a*S*)- and *rac*-(2*S*,4a*R*,8a*S*)-2-Phenoxy-1,2,3,4,4a,5,6,7,8,8a-decahydro-1,3,2-benzodiazaphosphinine 2-Oxides (14a and 14b)**

14a: $C_{13}H_{19}N_2O_2P$ (266.28): calcd. C 58.64, H 7.19, N 10.52; found C 58.86, H 7.38, N 10.43. MS: *m*/*z* = 266 $[M]^+$.

14b: $C_{13}H_{19}N_2O_2P$ (266.28): calcd. C 58.64, H 7.19, N 10.52; found C 58.79, H 6.98, N 10.40. MS: *m*/*z* = 266 $[M]^+$.

***rac*-(2*S*,4a*R*,8a*R*)- and *rac*-(2*R*,4a*R*,8a*R*)-3-Methyl-2-phenoxy-1,2,3,4,4a,5,6,7,8,8a-decahydro-1,3,2-benzodiazaphosphinine 2-Oxides (15a and 15b)**

15a: $C_{14}H_{21}N_2O_2P$ (280.30): calcd. C 59.99, H 7.55, N 9.99; found C 59.68, H 7.40, N 9.91. MS: *m*/*z* = 280 $[M]^+$.

15b: $C_{14}H_{21}N_2O_2P$ (280.30): calcd. C 59.99, H 7.55, N 9.99; found C 59.74, H 7.68, N 10.15. MS: *m*/*z* = 280 $[M]^+$.

***rac*-(2*S*,4a*R*,8a*S*)- and *rac*-(2*R*,4a*R*,8a*S*)-3-Methyl-2-phenoxy-1,2,3,4,4a,5,6,7,8,8a-decahydro-1,3,2-benzodiazaphosphinine 2-Oxides (16a and 16b):**

16a: $C_{14}H_{21}N_2O_2P$ (280.30): calcd. C 59.99, H 7.55, N 9.99; found C 59.71, H 7.69, N 9.72. MS: *m*/*z* = 280 $[M]^+$.

16b: $C_{14}H_{21}N_2O_2P$ (280.30): calcd. C 59.99, H 7.55, N 9.99; found C 59.78, H 7.33, N 10.12. MS: *m*/*z* = 280 $[M]^+$.

Table 9. Purification of the crude products **7**–**22** of the ring-closure reactions.[a]

	a:**b**[b]	A	B		C	Yield [g] (%)	D[c]	M.p. [°C]
7	[d]	8:2	**a**	**7a**	*n*-hexane	0.19 (11)	–	155–157
				7b	*n*-hexane	0.14 (8)	–	187–190
8	67:33	9:1	**b**	**8a**	Et_2O	0.18 (10)	–	180–184
				8b	Et_2O	0.33 (19)	EtOAc	174–176
9	68:32	15:1	**a**	**9a**	Et_2O	0.48 (26)	iPr_2O	87–89
				9b	Et_2O	0.22 (12)	mixt.	172–174
10	36:64	9:1	**b**	**10a**[e]	*n*-hexane	0.19 (10)	–	157–160
				10b	*n*-hexane	0.39 (21)	–	194–196
11	13:87	10:1	**a**	**11a**	*n*-hexane	0.22 (12)	–	146–149
				11b	*n*-hexane	0.19 (10)	–	155–159
12	55:45	9:1	**b**	**12a**	*n*-hexane	0.28 (15)	–	175–178
				12b	*n*-hexane	0.19 (10)	–	162–165
13	52:48	10:1	**a**	**13a**	*n*-hexane	0.41 (22)	mixt.	136–138
				13b	Et_2O	0.41 (22)	mixt.	129–131
14	50:50	9:1	**b**	**14a**	Et_2O	0.41 (22)	EtOAc	155–158
				14b	Et_2O	0.47 (25)	EtOAc	134–135
15	55:45	20:1	**a**	**15a**	*n*-hexane	0.57 (29)	iPr_2O	114–115
				15b	*n*-hexane	0.65 (33)	mixt.	109–111
16	49:51	20:1	**b**	**16a**	*n*-hexane	0.63 (32)	mixt.	132–134
				16b	*n*-hexane	0.65 (33)	mixt.	138–139
17	50:50	20:1	**a**	**17a**	*n*-hexane	0.71 (36)	mixt.	102–103
				17b	*n*-hexane	0.61 (31)	mixt.	123–124
18	50:50	15:1	**b**	**18a**	*n*-hexane	0.57 (29)	EtOAc	98–100
				18b	Et_2O	0.29 (15)	–	170–174
19	62:38	9:1	**a**	**19a**	*n*-hexane	0.64 (29)	–	139–140.5
				19b	*n*-hexane	0.57 (26)	–	133–136
20	[d]	7:1	–	[f]	–	–	–	–
21	43:57	7:3	**a**	**21a**	*n*-hexane	0.34 (15)	–	foam
				21b	*n*-hexane	0.39 (17)	–	153–156
22	50:50	9:1	**a**	**22a**	Et_2O	0.44 (19)	–	119–121
				22b	Et_2O	0.55 (24)	–	129–132

[a] Crude products containing both P epimers (with ratio **a**:**b**) were purified by column chromatography using ethyl acetate/methanol as eluent (solvent ratio = A). The more mobile (B) and less mobile diastereomers were crystallized by evaporation from their respective fractions and were filtered from solvent C to yield the diastereomers in pure form. For recrystallization, if necessary, solvent D was used. [b] As determined by ^{1}H NMR spectroscopy (^{31}P NMR for **9**). [c] mixt. = diisopropyl ether/ethyl acetate (3:1). [d] Not obtained owing to the presence of side-products and/or poor solubility in $CDCl_3$. [e] Contained **10b** as a minor impurity (ca. 4% by ^{1}H NMR). [f] Obtained only as a 76:24 mixture (**a**:**b**) of epimers after column chromatography.

***rac*-(2*R*,4a*R*,8a*R*)- and *rac*-(2*S*,4a*R*,8a*R*)-1-Methyl-2-phenoxy-1,2,3,4,4a,5,6,7,8,8a-decahydro-1,3,2-benzodiazaphosphinine 2-Oxides (17a and 17b)**

17a: $C_{14}H_{21}N_2O_2P$ (280.30): calcd. C 59.99, H 7.55, N 9.99; found C 59.69, H 7.68, N 9.78. MS: *m*/*z* = 280 $[M]^+$.

17b: $C_{14}H_{21}N_2O_2P$ (280.30): calcd. C 59.99, H 7.55, N 9.99; found C 60.17, H 7.38, N 10.08. MS: *m*/*z* = 280 $[M]^+$.

***rac*-(2*R*,4a*R*,8a*S*)- and *rac*-(2*S*,4a*R*,8a*S*)-1-Methyl-2-phenoxy-1,2,3,4,4a,5,6,7,8,8a-decahydro-1,3,2-benzodiazaphosphinine 2-Oxides (18a and 18b)**

18a: $C_{14}H_{21}N_2O_2P$ (280.30): calcd. C 59.99, H 7.55, N 9.99; found C 60.24, H 7.32, N 9.67. MS: *m*/*z* = 280 $[M]^+$.

18b: $C_{14}H_{21}N_2O_2P$ (280.30): calcd. C 59.99, H 7.55, N 9.99; found C 60.20, H 7.71, N 10.13. MS: *m*/*z* = 280 $[M]^+$.

***rac*-(2*S*,4a*R*,8a*R*)- and *rac*-(2*R*,4a*R*,8a*R*)-2-[Bis(2-chloroethyl) amino]-1,2,3,4,4a,5,6,7,8,8a-decahydro-1,3,2-benzodiazaphosphinine 2-Oxides (19a and 19b)**[35]

19a: $C_{11}H_{22}Cl_2N_3OP$ (314.19): calcd. C 42.05, H 7.06, N 13.37; found C 41.81, H 6.87, N 13.53. MS: *m*/*z* = 313 $[M]^+$.

19b: $C_{11}H_{22}Cl_2N_3OP$ (314.19): calcd. C 42.05, H 7.06, N 13.37; found C 42.21, H 6.80, N 13.04. MS: *m*/*z* = 313 $[M]^+$.

***rac*-(2*S*,4a*R*,8a*S*)- and *rac*-(2*R*,4a*R*,8a*S*)-2-[Bis(2-chloroethyl) amino]-1,2,3,4,4a,5,6,7,8,8a-decahydro-1,3,2-benzodiazaphosphinine 2-Oxides (20a and 20b):**[35] This compound was obtained as a 76:24 mixture of **20a** and **20b** (by ^{1}H NMR) of the epimers. $C_{11}H_{22}Cl_2N_3OP$ (314.19): calcd. C 42.05, H 7.06, N 13.37; found C 42.41, H 6.79, N 13.53. MS: *m*/*z* = 313 $[M]^+$.

***rac*-(2*R*,4a*R*,8a*R*)- and *rac*-(2*S*,4a*R*,8a*R*)-2-[Bis(2-chloroethyl) amino]-3-methyl-1,2,3,4,4a,5,6,7,8,8a-decahydro-1,3,2-benzodiazaphosphinine 2-Oxides (21a and 21b)**[35]

21a: $C_{12}H_{24}Cl_2N_3OP$ (328.22): calcd. C 43.91, H 7.37, N 12.80; found C 44.11, H 7.57, N 13.06. MS: *m*/*z* = 327 $[M]^+$.

21b: $C_{12}H_{24}Cl_2N_3OP$ (328.22): calcd. C 43.91, H 7.37, N 12.80; found C 43.74, H 7.22, N 12.99. MS: *m*/*z* = 327 $[M]^+$.

***rac*-(2*R*,4a*R*,8a*R*)- and *rac*-(2*S*,4a*R*,8a*R*)-2-[Bis(2-chloroethyl) amino]-1-methyl-1,2,3,4,4a,5,6,7,8,8a-decahydro-1,3,2-benzodiazaphosphinine 2-Oxides (22a and 22b)**[35]

22a: $C_{12}H_{24}Cl_2N_3OP$ (328.22): calcd. C 43.91, H 7.37, N 12.80; found C 44.18, H 7.48, N 12.72. MS: *m*/*z* = 327 $[M]^+$.

22b: $C_{12}H_{24}Cl_2N_3OP$ (328.22): calcd. C 43.91, H 7.37, N 12.80; found C 44.06, H 7.52, N 13.13. MS: *m*/*z* = 327 $[M]^+$.

Supporting Information (for details see the footnote on the first page of this article): ^{1}H, ^{13}C and ^{31}P NMR chemical shifts and

$J_{H,H}$, $J_{P,H}$ and $J_{P,C}$ coupling constants for compounds **7**–**22a**,**b**. Typical acquisition and processing parameters for the 1D and 2D NMR spectra. Cartesian coordinates and energies for the DFT optimized geometries of **10a** and **10b**.

Acknowledgments

Z. Z. is grateful to the Centre for International Mobility (CIMO), Finland for a grant. Dr. Petri Tähtinen is thanked for technical assistance with the DFT calculations.

[1] S. M. Ludeman in *Biomedical Chemistry* (Ed.: P. F. Torrence), Wiley-Interscience, New York, **2000**, pp. 163–187.
[2] K. Afarinkia, A. J. Twist, H. Yu, *J. Org. Chem.* **2004**, *69*, 6500–6503.
[3] R. Pedrosa, A. Maestro, A. Pérez-Encabo, R. Raliegos, *Synlett* **2004**, 1300–1302.
[4] Z. Zalán, T. A. Martinek, L. Lázár, F. Fülöp, *Tetrahedron* **2003**, *59*, 9117–9125, and references cited therein.
[5] O. M. Friedman, E. Boger, V. Grubliauskas, H. Sommer, *J. Med. Chem.* **1963**, *6*, 50–58.
[6] S. E. Denmark, S. Fujimori, *Org. Lett.* **2002**, *4*, 3473–3476.
[7] S. E. Denmark, S. Fujimori, *Org. Lett.* **2002**, *4*, 3477–3480.
[8] S. E. Denmark, D. M. Coe, N. E. Pratt, B. D. Griedel, *J. Org. Chem.* **1994**, *59*, 6161–6163.
[9] S. E. Denmark, J.-H. Kim, *Can. J. Chem.* **2000**, *78*, 673–688.
[10] B. Burns, N. P. King, H. Tye, J. R. Studley, M. Gamble, M. Wills, *J. Chem. Soc., Perkin Trans. 1* **1998**, 1027–1038.
[11] S. E. Denmark, R. L. Dorow, *J. Am. Chem. Soc.* **1990**, *112*, 864–866.
[12] T. Viljanen, P. Tähtinen, K. Pihlaja, F. Fülöp, *J. Org. Chem.* **1998**, *63*, 618–627.
[13] H. Kivelä, Z. Zalán, P. Tähtinen, R. Sillanpää, F. Fülöp, K. Pihlaja, *Eur. J. Org. Chem.* **2005**, 1189–1200.
[14] S. E. Denmark, X. Su, Y. Nishigaichi, D. M. Coe, K.-T. Wong, S. B. D. Winter, J. Y. Choi, *J. Org. Chem.* **1999**, *64*, 1958–1967.
[15] K. Pihlaja, F. Fülöp, J. Mattinen, G. Bernáth, *Acta Chem. Scand., Ser. B* **1987**, *41*, 228–231.
[16] L. Lázár, A. Göblyös, T. A. Martinek, F. Fülöp, *J. Org. Chem.* **2002**, *67*, 4734–4741.
[17] D. G. Gorenstein, *Prog. Nucl. Magn. Reson. Spectrosc.* **1983**, *16*, 1–98.
[18] G. S. Bajwa, S. Chandrasekaran, J. H. Hargis, A. E. Sopchik, D. Blatter, W. G. Bentrude, *J. Am. Chem. Soc.* **1982**, *104*, 6385–6392.
[19] K. Taira, K. Lai, D. G. Gorenstein, *Tetrahedron* **1986**, *42*, 229–238.
[20] V. M. S. Gil, W. von Philipsborn, *Magn. Reson. Chem.* **1989**, *27*, 409–430.
[21] J.-C. Yang, D. O. Shah, N. U. M. Rao, W. A. Freeman, G. Sosnovsky, D. G. Gorenstein, *Tetrahedron* **1988**, *44*, 6305–6314.
[22] K. Pihlaja, E. Kleinpeter, *Carbon-13 NMR Chemical Shifts in Structural and Stereochemical Analysis*, VCH Publishers, New York, **1994**, p. 58.
[23] R. K. Harris, E. D. Becker, S. M. Cabral de Menezes, R. Goodfellow, P. Granger, *Pure Appl. Chem.* **2001**, *73*, 1795–1818.
[24] See for example: R. Laatikainen, M. Niemitz, U. Weber, J. Sundelin, T. Hassinen, J. Vepsäläinen, *J. Magn. Reson., Ser. A* **1996**, *120*, 1–10; home page: http://www.perchsolutions.com.
[25] M. J. Frisch, G. W. Trucks, H. B. Schlegel, G. E. Scuseria, M. A. Robb, J. R. Cheeseman, V. G. Zakrzewski, J. A. Montgomery Jr, R. E. Stratmann, J. C. Burant, S. Dapprich, J. M. Millam, A. D. Daniels, K. N. Kudin, M. C. Strain, O. Farkas, J. Tomasi, V. Barone, M. Cossi, R. Cammi, B. Mennucci, C. Pomelli, C. Adamo, S. Clifford, J. Ochterski, G. A. Petersson, P. Y. Ayala, Q. Cui, K. Morokuma, P. Salvador, J. J. Dannenberg, D. K. Malick, A. D. Rabuck, K. Raghavachari, J. B. Foresman, J. Cioslowski, J. V. Ortiz, A. G. Baboul, B. B. Stefanov, G. Liu, A. Liashenko, P. Piskorz, I. Komaromi, R. Gomperts, R. L. Martin, D. J. Fox, T. Keith, M. A. Al-Laham, C. Y. Peng, A. Nanayakkara, M. Challacombe, P. M. W. Gill, B. G. Johnson, W. Chen, M. W. Wong, J. L. Andres, C. Gonzalez, M. Head-Gordon, E. S. Replogle, J. A. Pople, *Gaussian 98, revision A.11*, Gaussian, Inc., Pittsburgh PA, **2001**.
[26] J. B. Foresman, Æ. Frisch, *Exploring Chemistry with Electronic Structure Methods*, 2nd ed., Gaussian Inc., Pittsburgh PA, **1996**, p. 64.
[27] A. D. Becke, *Phys. Rev. A* **1988**, *38*, 3098–3100.
[28] A. D. Becke, *J. Chem. Phys.* **1993**, *98*, 5648–5652.
[29] C. Lee, W. Yang, R. G. Parr, *Phys. Rev. B* **1988**, *37*, 785–789.
[30] V. G. Malkin, O. L. Malkina, D. R. Salahub, *Chem. Phys. Lett.* **1994**, *221*, 91–99.
[31] P. Tähtinen, A. Bagno, A. Koch, K. Pihlaja, *Eur. J. Org. Chem.* **2004**, 4921–4930.
[32] K. Okamoto, M. Noji, Y. Kidani, *Bull. Chem. Soc. Jpn.* **1981**, *54*, 713–718.
[33] W. L. F. Armarego, P. A. Reece, *J. Chem. Soc., Perkin Trans. 1* **1974**, 2313–2319.
[34] W. L. F. Armarego, T. Kobayashi, *J. Chem. Soc. (C)* **1971**, 238–245.
[35] In this study, compounds **19**–**22a**,**b** are named as 2-[bis(2-chloroethyl)amino]-substituted 1,3,2-benzodiazaphosphinine 2-oxides to provide uniformity with the nomenclature for the 2-phenyl and 2-phenoxy derivatives. The correct IUPAC name, for example, for **19a** would be *rac*-(2*S*,4a*R*,8a*R*)-*N*,*N*-bis(2-chloroethyl)decahydro-1,3,2-benzodiazaphosphinin-2-amine 2-oxide.

Received: September 1, 2005
Published Online: March 1, 2006

